

NO-A192 329

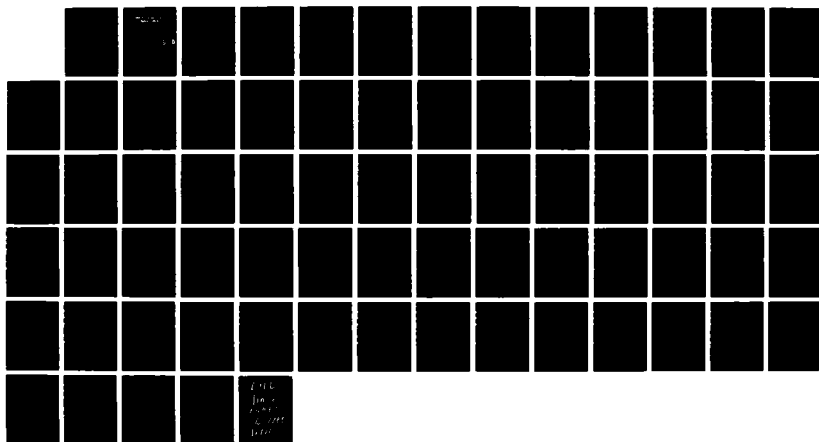
VIBRATION RESPONSE OF CONSTRAINED VISCOELASTICALLY
DAMPED PLATES: ANALYSES AND EXPERIMENTS(U) NAVAL
POSTGRADUATE SCHOOL MONTEREY CA G J MAURER DEC 87

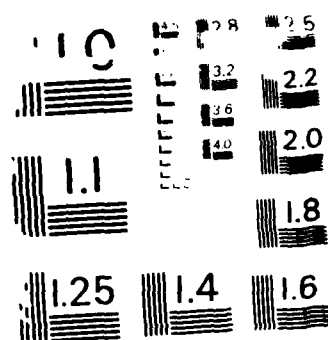
1/1

UNCLASSIFIED

F/G 28/11

NL





U.S. GOVERNMENT PRINTING OFFICE: 1963
NATIONAL BUREAU OF STANDARDS - 1963

AD-A192 329

DTIC FILE CODE

2

NAVAL POSTGRADUATE SCHOOL Monterey, California



THESIS

DTIC
ELECTE
MAY 05 1988
S D
a
E

VIBRATION RESPONSE OF CONSTRAINED
VISCOELASTICALLY DAMPED PLATES:
ANALYSES AND EXPERIMENTS

by

Gerald J. Maurer

December 1987

Thesis Advisor:

Young S. Shin

Approved for public release; distribution is unlimited

30 5 4 008

REPORT DOCUMENTATION PAGE

1a. REPORT SECURITY CLASSIFICATION UNCLASSIFIED			1b. RESTRICTIVE MARKINGS	
2a. SECURITY CLASSIFICATION AUTHORITY			3. DISTRIBUTION / AVAILABILITY OF REPORT Approved for public release; distribution is unlimited	
2b. DECLASSIFICATION / DOWNGRADING SCHEDULE				
4. PERFORMING ORGANIZATION REPORT NUMBER(S)			5. MONITORING ORGANIZATION REPORT NUMBER(S)	
6a. NAME OF PERFORMING ORGANIZATION Naval Postgraduate School		6b. OFFICE SYMBOL (If applicable) Code 69	7a. NAME OF MONITORING ORGANIZATION Naval Postgraduate School	
6c. ADDRESS (City, State, and ZIP Code) Monterey, California 93943-5000			7b. ADDRESS (City, State, and ZIP Code) Monterey, California 93943-5000	
8a. NAME OF FUNDING / SPONSORING ORGANIZATION		8b. OFFICE SYMBOL (If applicable)	9. PROCUREMENT INSTRUMENT IDENTIFICATION NUMBER	
8c. ADDRESS (City, State, and ZIP Code)			10. SOURCE OF FUNDING NUMBERS	
			PROGRAM ELEMENT NO.	PROJECT NO.
11. TITLE (Include Security Classification) VIBRATION RESPONSE OF CONSTRAINED VISCOELASTICALLY DAMPED PLATES: ANALYSES AND EXPERIMENTS				
12. PERSONAL AUTHOR(S) Maurer, Gerald J.				
13a. TYPE OF REPORT Master's Thesis		13b. TIME COVERED FROM _____ TO _____		14. DATE OF REPORT (Year, Month, Day) 1987, December
15. PAGE COUNT 72				
16. SUPPLEMENTARY NOTATION				
17. COSATI CODES			18. SUBJECT TERMS (Continue on reverse if necessary and identify by block number) Viscoelastic Material; Modal Strain Energy Method; Composite Frequency Response Curves <i>The 2000</i>	
FIELD	GROUP	SUB-GROUP		
19. ABSTRACT (Continue on reverse if necessary and identify by block number) <p>The frequency response analysis of several constrained viscoelastically damped plates were performed with modifications to account for the frequency dependent properties of viscoelastic materials (loss factors and shear modulus) using MSC/NASTRAN. A modal strain energy approximation method was also applied to each plate. Comparisons of the frequency response analysis to the modal strain energy method were made for each plate structure. The experiments were performed on the plates to establish the base line data for the comparisons.</p> <p>The modal strain energy method frequency response plots showed good agreement with the frequency response analysis method plots for all plate structures analyzed. Plate structures with fewer natural frequencies in the frequency range investigated showed better agreement between the two prediction methods than the structures with more natural frequencies. The</p>				
20. DISTRIBUTION / AVAILABILITY OF ABSTRACT <input checked="" type="checkbox"/> UNCLASSIFIED/UNLIMITED <input type="checkbox"/> SAME AS RPT. <input type="checkbox"/> DTIC USERS			21. ABSTRACT SECURITY CLASSIFICATION Unclassified	
22a. NAME OF RESPONSIBLE INDIVIDUAL Professor Young S. Shin			22b. TELEPHONE (Include Area Code) (408) 646-2568	22c. OFFICE SYMBOL Code 69Sg

#19 - ABSTRACT - (CONTINUED)

experimental data for the plate analyzed indicate less damping than calculated by either of the finite element prediction methods. The experimentally determined natural frequency modes were well approximated by both of the finite element prediction methods.

Accession For	
NTIS GRA&I	<input checked="checked" type="checkbox"/>
DTIC TAB	<input type="checkbox"/>
Unannounced	<input type="checkbox"/>
Justification	
By	
Distribution/	
Availability Codes	
Dist	Avail and/or Special
A-1	

Approved for public release; distribution is unlimited

Vibration Response of Constrained Viscoelastically
Damped Plates: Analyses and Experiments

by

Gerald J. Maurer
Lieutenant, United States Navy
B.S., University of Minnesota, 1981

Submitted in partial fulfillment of the
requirements for the degree of

MASTER OF SCIENCE IN MECHANICAL ENGINEERING


from the

NAVAL POSTGRADUATE SCHOOL
December 1987

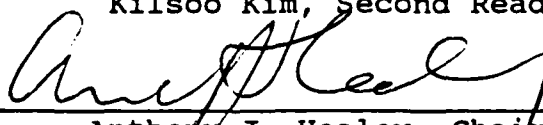
Author:



Gerald J. Maurer

Approved by:


Young S. Shin, Thesis Advisor


Kilsoo Kim, Second Reader


Anthony J. Healey, Chairman,
Department of Mechanical Engineering


Gordon E. Schacher,
Dean of Science and Engineering

ABSTRACT

The frequency response analysis of several constrained viscoelastically damped plates were performed with modifications to account for the frequency dependent properties of viscoelastic materials (loss factors and shear modulus) using MSC/NASTRAN. A modal strain energy approximation method was also applied to each plate. Comparisons of the frequency response analysis to the modal strain energy method were made for each plate structure. The experiments were performed on the plates to establish the base line data for the comparisons.

The modal strain energy method frequency response plots showed good agreement with the frequency response analysis method plots for all plate structures analyzed. Plate structures with fewer natural frequencies in the frequency range investigated showed better agreement between the two prediction methods than the structures with more natural frequencies. The experimental data for the plate analyzed indicate less damping than calculated by either of the finite element prediction methods. The experimentally determined natural frequency modes were well approximated by both of the finite element prediction methods.

TABLE OF CONTENTS

I.	INTRODUCTION -----	1
II.	THEORY AND BACKGROUND -----	3
III.	MATERIALS AND METHODS -----	9
	A. MODEL DESCRIPTION -----	9
	B. DESIGN OF VISCOELASTIC AND CONSTRAINING LAYER THICKNESSES -----	9
	C. VISCOELASTIC MATERIAL -----	11
	D. NASTRAN FINITE ELEMENT MODEL -----	14
	1. Modal Strain Energy (MSE) Method -----	14
	2. Frequency Response Method -----	17
	E. VIBRATION GENERATOR TESTING ARRANGEMENT -----	18
IV.	RESULTS -----	29
	A. SIMPLE PLATE -----	29
	B. MILLED PLATE, FREE CONSTRAINING LAYER -----	30
	C. MILLED PLATE WITH WELDED CONSTRAINING LAYER -	31
V.	CONCLUSIONS -----	39
VI.	RECOMMENDATIONS -----	43
APPENDIX A:	NOMOGRAM LOSS FACTOR AND SHEAR MODULUS CALCULATIONS -----	44
APPENDIX B:	MSC/NASTRAN CODE FOR SIMPLE PLATE NORMAL MODE ANALYSIS AND MSC/NASTRAN CODE FOR SIMPLE PLATE FREQUENCY RESPONSE ANALYSIS -----	49
	LIST OF REFERENCES -----	60
	INITIAL DISTRIBUTION LIST -----	62

LIST OF FIGURES

2.1	Variation of Shear Modulus and Loss Factor with Temperature -----	8
3.1	Dimensions of Simple Plate with Applied Viscoelastic and Constraining Layers -----	20
3.2	Dimensions of Milled Plate with Applied Viscoelastic and Constraining Layers -----	21
3.3	Estimate of System Loss Factor of the Simple Plate with Varying Thicknesses of Viscoelas- tic Damping and Constraining Layers -----	22
3.4	Loss Factor Variation of ISD-112 with Varying Frequency and Temperature -----	23
3.5	University of Dayton Nomogram for 3M ISD-112 Damping Material -----	24
3.6	MSC/NASTRAN Finite Element Model for Simple Plate -----	25
3.7	MSC/NASTRAN Finite Element Model for Milled Plate with Free Constraining Layer -----	26
3.8	MSC/NASTRAN Finite Element Model for Milled Plate with Welded Constraining Layer -----	27
3.9	Iterate Technique for the Simple Plate Modes ----	28
4.1	Simple Plate, Experimental Data Before and After Application of Viscoelastic Damping Treatment -----	32
4.2	Milled Plate with Free Constraining Layer, Experimental Data Before and After Applica- tion of Viscoelastic Damping Treatment -----	33
4.3	Welded Plate with Welded Constraining Layer, Experimental Data Before and After Applica- tion of Viscoelastic Damping Treatment -----	34
4.4	Simple Damped Plate, Experimental Data and Two Predictions Method Curves -----	35
4.5	Milled Damped Plate with Free Constraining Layer, Experimental Data and Two Predictions Method Curves -----	36

4.6	Milled Damped Plate with Welded Constraining Layer, Two Predictions Method Curves -----	37
4.7	Milled Damped Plate Experimental Data Before Welding Constraining Layer and After Cutting Weld -----	38
A.1	FORTTRAN Program to Calculate the Viscoelastic Material Shear Modulus, Loss Factor and System Loss Factor (Page One) -----	45
A.2	FORTTRAN Program to Calculate the Viscoelastic Material Shear Modulus, Loss Factor and System Loss Factor (Page Two) -----	46
A.3	FORTTRAN Program to Calculate the Viscoelastic Material Shear Modulus, Loss Factor and System Loss Factor (Page Three) -----	47
A.4	FORTTRAN Program to Calculate the Viscoelastic Material Shear Modulus, Loss Factor and System Loss Factor (Page Four) -----	48
B.1	MSC/NASTRAN Normal Mode Analysis of the Simple Plate (Page One) -----	50
B.2	MSC/NASTRAN Normal Mode Analysis of the Simple Plate (Page Two) -----	51
B.3	MSC/NASTRAN Normal Mode Analysis of the Simple Plate (Page Three) -----	52
B.4	MSC/NASTRAN Normal Mode Analysis of the Simple Plate (Page Four) -----	53
B.5	MSC/NASTRAN Normal Mode Analysis of the Simple Plate (Page Five) -----	54
B.6	MSC/NASTRAN Frequency Response Analysis of the Simple Plate (Page One) -----	55
B.7	MSC/NASTRAN Frequency Response Analysis of the Simple Plate (Page Two) -----	56
B.8	MSC/NASTRAN Frequency Response Analysis of the Simple Plate (Page Three) -----	57
B.9	MSC/NASTRAN Frequency Response Analysis of the Simple Plate (Page Four) -----	58
B.10	MSC/NASTRAN Frequency Response Analysis of the Simple Plate (Page Five) -----	59

ACKNOWLEDGMENTS

The author would like to express his appreciation for the guidance extended by Prof. Young Shin and Dr. Kilsoo Kim. Their patience and friendship made the learning of a complex subject much easier. The author would also like to gratefully acknowledge the continued support provided by Dr. P. Mahmoodi and the personnel at the 3M Corporate Research Laboratories, Saint Paul, Minnesota, who provided materials and suggestions for the research contained in the thesis.

I. INTRODUCTION

Advances in the material sciences area have resulted in metals with high strength to weight ratios. The application of such material can result in structures with low levels of damping. Exposure of these structures to high levels of excitation creates a need for damping techniques which are both inexpensive and effective. Introduction of a distributed viscoelastic material with an incorporated constraining layer has gained widespread acceptance as a means of reducing vibration response. Many finite element codes have been developed which incorporate frequency prediction methods for use in design applications, reducing the need for experimental analysis. However, accurate behavioral predictions of applied viscoelastic material have remained costly, due to the frequency and temperature dependence in viscoelastic materials.

The response of the simplest structures can be represented by continuous classical methods but the finite element approach remains the method of choice when complex physical systems must be analyzed. The use of a finite element method to find the system response requires modifications to capture the environmental dependencies of the applied viscoelastic layer. One standard method of conducting a frequency analysis of dampened structures is

through repeated application of the frequency response analysis over incremented steps in frequency. A second approach, using modal strain energy approximations in conjunction with the finite element method, has proved effective in predicting excitation responses of structures with a constrained viscoelastic layer. This paper investigates the two prediction methods described above as applied to plate structures. MSC/NASTRAN was chosen for the analyses because of its widespread availability and previous use in this area. The prediction methods were applied to two plate structures, one with the damping material having edge exposure to the environment and a similar plate with the damping material protected from the environment and possible corrosion, through the use of an edge weld. The edge-welded plate was evaluated before and after welding to determine possible damage to the viscoelastic layer. The prediction methods were evaluated for ease of application and prediction accuracy as compared to the experimental data.

II. THEORY AND BACKGROUND

Continuous structures in the physical world possess distributed characteristics of mass, damping and stiffness. [Ref. 1:pp. 140-141] Structures with such characteristics are said to contain an infinite number of degrees of freedom. The classical vibration analysis of such a continuous system involves the construction of a discrete mathematical model with a finite number of parameters to approximate the overall system response. Construction of a model of N discrete elements allows the discretized continuous system to be represented by the coupled matrix equations:

$$[M]\{\ddot{q}(t)\} + [C]\{\dot{q}(t)\} + [K]\{q(t)\} = \{Q(t)\} \quad (2.1)$$

Linear transformation and normalization of the undamped portion of Equation (2.1) and assumption of damping approximated by an appropriate diagonal matrix gives the uncoupled equations:

$$\{\ddot{\alpha}(t)\} + [2\zeta\omega_n]\{\dot{\alpha}(t)\} + [\omega_n^2]\{\alpha(t)\} = \{1(t)\} \quad (2.2)$$

$$\{q(t)\} = [\phi]\{\alpha(t)\} \quad (2.3)$$

where:

$\{q(t)\}$ = displacement vector

$[\phi]$ = mode shape matrix

$[\omega_n^2]$ = vector of natural frequencies

ζ = damping factor

$\{l(t)\}$ = transformed matrix of applied loads.

Application of modal analysis through developed finite element codes have resulted in readily obtainable solutions to Equations (2.2) and (2.3) for complicated, lightly damped structures. [Ref. 2:Secs. 2.3,4.3.2; Ref. 3:p. 2] Recently, viscoelastic materials have been added to structures to improve their overall damping characteristics. However, the addition of these viscoelastic materials to design structures introduce both frequency and temperature dependent variables that must be incorporated into the finite element analysis. [Ref. 4:p. 2]

Viscoelastic damping has been observed in many polymeric materials and has been directly attributed to the relaxation and recovery of long carbon atom chains of the polymer after deforming. [Ref. 5:p. 67] Because of their effect on molecular motion, temperature and frequency influence these "relaxation and recovery" properties. Thus, a complete understanding of the temperature and frequency dependent behavior of the material is essential.

Moderate changes in temperature or large changes in frequency result in definite predictable alterations in the viscoelastic material properties of shear modulus of elasticity and loss factor. Actual quantitative changes in the damping properties vary substantially with the chosen material. Qualitative changes are categorized into three descriptive regions; the glassy regions, transition region, and the rubbery region as shown in Figure 2.1. In a given viscoelastic material, all three regions are typically contained in two to three decades of frequency. [Ref. 5:p. 91]

Damping at relatively low temperatures for the given material is in the glassy region and exhibits a low loss factor and high shear modulus of elasticity. As the material temperature is increased the shear modulus begins to drop slowly as the loss factor rises. Sufficient temperature increases allow the damping material to enter the transition region, characterized by a rapidly decreasing shear modulus value. The loss factor reaches a peak value at the maximum rate of change in shear modulus value. Further increases in temperature result in the material entering the rubbery region with a corresponding decrease in loss factor and shear modulus values. While the above discussion is descriptive of varying properties with temperature increases, it also applies to frequency decreases. Examination of several materials shows a 25

degree fahrenheit increase being roughly equivalent to a one decade frequency decrease. For example, a 25° F increased temperature is roughly equivalent to a 10 kHz to 1 kHz or a 1000 Hz-100 Hz drop in frequency. [Ref. 6:pp. A1-A21]

The high sensitivity of viscoelastic materials causes the matrix values of Equation (2.2) to change with only mild variations in excitation and environmental conditions. This results in finite element solutions that are only applicable over a narrow range of frequency or temperature. A solution to Equations (2.2) and (2.3) which reflects varying matrix values may thus be obtained by the segmentation of the equations into incremental modal frequency response finite element analyses steps. This composite approach gives good results but in practical applications may become prohibitively expensive and time consuming, especially when several design alternatives are under consideration.

An application of the modal strain energy method (MSE) by Johnson and Kienholz [Ref. 7:pp. 5-12] is suggested as an alternative solution to Equations (2.2) and (2.3) by imposing frequency dependency on the frequency response through post analysis data manipulation. In the MSE approach, the MSC/NASTRAN code is used to construct a finite element model with constant, midrange values of loss factor and shear modulus of elasticity. NASTRAN modal analysis is applied and the mode shapes and natural frequencies are extracted and inserted into Equations (2.2) and (2.3). The

fraction of elastic strain energy attributed to the viscoelastic core at each natural frequency is also obtained from the modal analysis and the damping material loss factors interpolated at each natural frequency. The matrix $[2\zeta\omega_n]$ of Equation (2.2) is then replaced with $[\eta(\frac{V_V}{V_T})\omega_n]$ when Equations (2.2) and (2.3) are modified using the interpolated loss factors, the frequency response solution becomes frequency dependent. The MSE method thus gives accurate solutions over a large frequency range while remaining cost effective.

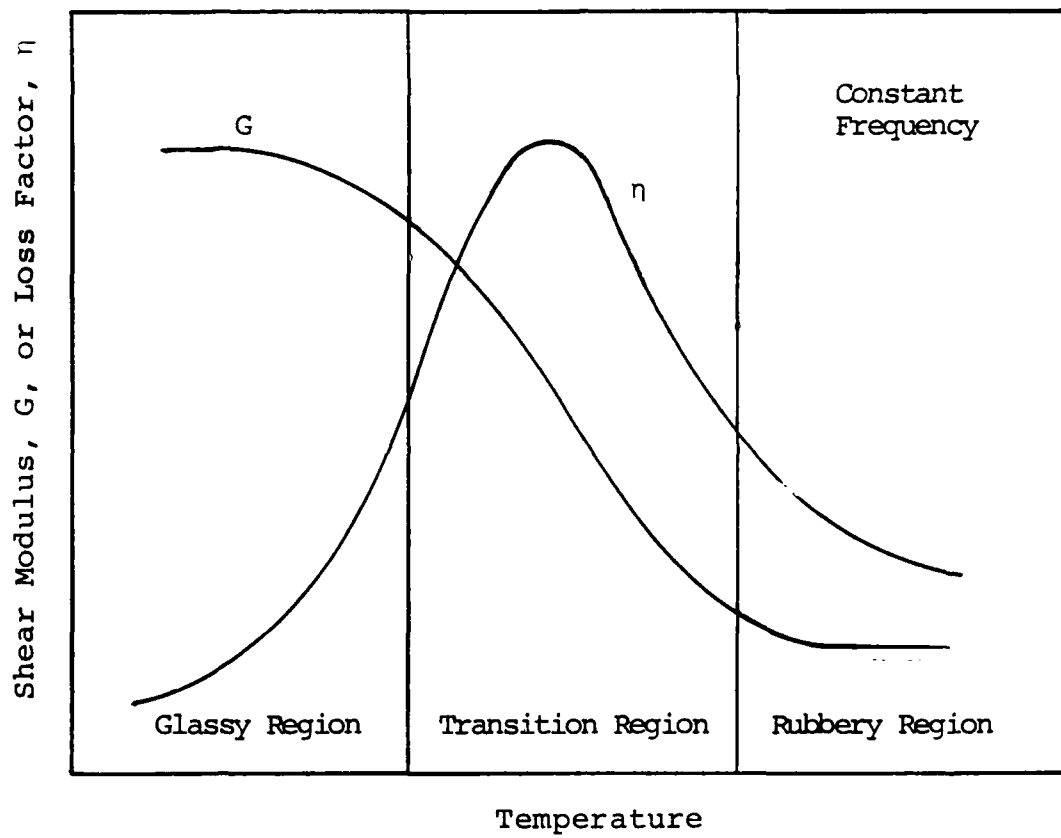


Figure 2.1 Variation of Shear Modulus and Loss Factor with Temperature [Ref. 5:p. 90]

III. MATERIAL AND METHODS

A. MODEL DESCRIPTION

Three different plate structures were analyzed during this study in order to provide a basis for the comparison with the finite element results. These plate structures consisted of a simple plate, a milled plate with an unrestricted constraining layer and finally a milled plate with a restricted constraining layer. The simple plate was a 14 x 30 inch aluminum rectangular plate, 3/8 inch thick (Figure 3.1). Dimensions were chosen to give approximately 15 resonant frequencies under 1000 Hz. The milled base plate and its dimensions are shown in Figure 3.2. All plates were machined from standard 6061 T6 aluminum. The use of a damped plate structure in a corrosive environment requires design modifications to protect the viscoelastic material. The welded plate structure of Figure 3.2 is such a design using the same material and overall thickness as the simple plate. This milled plate was subjected to vibration analysis before and after welding to detect reduced damping due to the welding process.

B. DESIGN OF VISCOELASTIC AND CONSTRAINING LAYER THICKNESSES

To approximate system loss factor, the plate structure was represented by a three layer beam system and subjected

to the Bernoulli-Euler type analysis described by M.L. Drake and developed by Ross, Kerwin, and Ungar [Ref. 8:pp. 1-6; Ref. 9]. The viscoelastic material and constraining layers were varied incrementally in the Bernoulli-Euler equations (3.1) to (3.3) below, using the FORTRAN program listed in Appendix A.

$$EI = \frac{E_1 H_1^3}{12} + \frac{E_2 H_2^3}{12} + \frac{E_3 H_3^3}{12} + E_1 H_1 D^2 + E_2 H_2 (H_{21} - D)^2 + E_3 H_3 (H_{31} - D)^2 - \left[\frac{E_2 H_2^2}{12} + \frac{E_2 H_2}{2} (H_{21} - D) + E_3 H_3 (H_{31} - D) \right] \frac{H_{31} - D}{1+g} \quad (3.1)$$

$$D = \frac{\frac{E_2 H_2}{2} (H_{21} - \frac{H_{31}}{2}) + g (E_2 H_2 H_{21} + E_3 H_3 H_{31})}{E_1 H_1 + \frac{E_3 H_2}{2} + g (E_1 H_1 + E_2 H_2 + E_3 H_3)} \quad (3.2)$$

$$H_{21} = \frac{H_1 + H_2}{2}; \quad H_{31} = \frac{H_1 + 2H_2 + H_3}{2}; \quad \text{and} \quad g = \frac{G_2}{E_3 H_3 H_2 K^2} \quad (3.3)$$

where:

E = Young's modulus of elasticity.

G = shear modulus.

I = second moment of area.

H = thickness.

$$K^2 = \left[\left(\frac{\text{Beam Approximation Length}}{\text{Plate Length}} \right)^2 + \left(\frac{\text{Beam Approximation Width}}{\text{Plate Width}} \right)^2 \right] \pi$$

and

Subscript 1 refers to the base structure.

Subscript 2 refers to the damping layer.

Subscript 3 refers to the outer layer.

No subscript refers to the composite system.

The maximum system loss factor and the temperature at which it occurred were found for each step. The results of 70 incremental thickness changes were plotted in Figure 3.3.

The University of Dayton Research Institute, in suggesting damping design procedures, recommends a system loss factor of 0.1 for most applications. [Ref. 10] Because Equations (3.1)-(3.3) are only an approximation, the desired system loss factor was increased to 0.3 in this analysis. From this figure and based on a loss factor of .3, the values of the viscoelastic damping layer and constraining layer were chosen to be .0625 and .25 inches respectively.

C. VISCOELASTIC MATERIAL

The damping material applied to all three models tested was 3M SJ-201 ISD-112 viscoelastic compound with a thickness of 60 mil, supplied with suitable adhesive already applied to both sides by the manufacturer, 3M, St. Paul, Minnesota. During application of the viscoelastic and constraining layers, care was taken to allow air to escape from between the layers. Entrapped air can result in severe bond defects

giving lower natural frequencies and reduced system loss factor. [Ref. 11:pp. 8-9]

ISD-112 was chosen for its excellent loss factor and shear modulus characteristics in the zero to 100° F temperature range for frequencies below 2,000 Hz. This trait is exhibited by the broad loss factor curve of Figure 3.4 and is highly desirable in many applications. Figure 3.5 shows a University of Dayton nomogram of the experimental determined shear modulus and loss factor properties for ISD-112. To determine shear modulus and loss factor values, locate the material temperature on the top of Figure 3.5 and the frequency of interest on the right margin. The diagonal line of temperature and horizontal line of frequency intersect on the vertical line of reduced frequency. Reduced frequency is the frequency value of interest multiplied by the temperature of interest and divided by the reference temperature of Figure 3.5. Reduced frequency and reference temperature are used to convert the input values of temperature and frequency to the conditions used to plot the loss factor and shear modulus curves. [Ref. 12:pp. 47-50] The intersection of reduced frequency and the plotted curves give the horizontal line of loss factor and shear modulus shown in the left margin. While nomograms are useful in comparing characteristics when selecting a damping material, precise values are difficult to read on the log-log scale and the actual equations of the

nomogram curves were used to give accurate values of loss factor and shear modulus in the finite element codes. The equations for ISD-112 are given below and used in the program listed in Appendix A. [Ref. 9:pp. 6-14]

$$\text{Log}(\text{FR}) = \log(\text{F}) - 12 * (\text{T} - \text{TZERO}) / (525 * \text{T} - \text{TZERO}) \quad (3.4)$$

$$\text{Log}(\text{G}) = \text{Log}(\text{ML}) + (2 * \text{Log } 10(\text{MROM}/\text{ML})) / (1 + \text{FROM}/\text{FR})^{\text{N}} \quad (3.5)$$

$$\text{Log}(\text{ETA}) = \text{Log}(\text{ETAFRO}) + \text{A} * \text{B} + \text{D} * (1 - \text{SQRT}(1 + \text{A}^2)) / (\text{C}/2) \quad (3.6)$$

where the ISD-112 viscoelastic material nomogram constants are:

TZERO = 131
 FROM = 400,000
 MROM = 2059.5
 N = .27
 ML = 28.427
 ETAFRO = 1.25
 SL = 0.27
 SH = -0.35
 FROL = 150,000
 C = 1.3

and:

FR = reduced frequency
 F = frequency

T = temperature
 G = shear modulus
 ETA = loss factor
 A = $(\text{Log}(\text{FR}) - \text{Log}(\text{FROL}))/C$
 B = $SL+SH$
 D = $SL-SH$

D. NASTRAN FINITE ELEMENT MODEL

Computer analysis of the sandwich structure was performed using the MSC/NASTRAN finite element program. As shown in Figures 3.6-3.8 the base plate and constraining layer were constructed of QUAD4 plate elements with 3/16 and 1/8 inch offsets, respectively. The more complicated HEXA8 solid elements used to simulate the sandwiched viscoelastic layer were required to accurately represent the strain energy due to shearing of the viscoelastic core and to account for the coupling between stretching and bending deformations. [Ref. 7:p. 8; Ref. 13:Sec. 2.22,4.3] The support bulk data card was used to give free-free end conditions to the plates. After constructing the finite element models, two different analyses were performed to predict frequency response amplitude.

1. Modal Strain Energy (MSE) Method

Rearranging Equations (2.2) and (2.3) and solving for the response amplitude gives the following equation:

$$x(\omega) = \left(\left(\sum_{i=1}^N \frac{\{1 - (\omega/\omega_n)^2\} (\phi_{E,i} \phi_{R,i} L) / \omega_n^2}{\{1 - (\omega/\omega_n)^2\}^2 + \{\eta_i (\frac{V_V}{V_T})_i (\omega/\omega_{n,i})\}^2} \right)^2 + \sum_{i=1}^N \frac{\{\eta_i (\frac{V_V}{V_T})_i (\omega/\omega_{n,i})\} (\phi_{E,i} \phi_{R,i} L) / \omega_n^2}{\{1 - (\omega/\omega_n)^2\}^2 + \{\eta_i (\frac{V_V}{V_T})_i (\omega/\omega_{n,i})\}^2} \right)^2 \right)^{1/2}$$

where:

$X(\omega)$ = amplitude of response as a function of frequency

$\omega_{n,i}$ = ith natural radian frequency

$\phi_{E,i}$ = mode shape value for the excitation grid point at the ith natural frequency

$\phi_{R,i}$ = mode shape value for the response grid point at the ith natural frequency

η_i = iterated viscoelastic material loss factor

$(V_V/V_T)_i$ = fraction of elastic strain in the viscoelastic material at each model

L = magnitude of the load applied at the excitation grid point.

The MSE method utilizes the MSC/NASTRAN method to find the constant values on the right side of Equation (3.7). The response amplitude is then calculated external to the finite element code. The mode shapes, natural frequencies and fractions of elastic strain energy in Equation (3.7) were determined using a single MSC/NASTRAN normal mode analysis for each plate. The damping material properties input to the MSC/NASTRAN normal analysis must be constant and were determined using the nomogram Equations (3.4)-(3.6) for a temperature of 60° F and the mid-range frequency of 500 Hz. The output of the MSC/NASTRAN normal analysis gave the

natural frequency, mode shapes, and the fractions of strain energy in the damping material at each associated natural frequency. The simple plate MSC/NASTRAN normal analysis program is listed in Appendix B.

The loss factor of Equation (3.7) is sensitive to the natural frequency and several MSC/NASTRAN mode analyses must be applied to compensate for errors in the derived natural frequencies. Johnson and Kienholz describe an iterative method to approximate this loss factor frequency sensitivity. [Ref. 7:pp. 27-31] The iterative method was applied by first plotting the damping materials shear modulus as a function of frequency using the nomogram Equations (3.4)-(3.6). The damping material shear modulus of each plate was then varied through several MSC/NASTRAN modal analyses and the resulting change in each natural frequency was plotted on the same curve. The intersection of the curves gives an approximation of the natural frequency and shear modulus for each mode. Figure 3.9 illustrates the iterate technique for two of the simple plate modes. The loss factor value was then found from this approximate shear modulus using the nomogram Equations (3.4)-(3.6). When this iterative method was first applied by Johnson and Kienholz, they noted the results differed from those observed in frequency response methods. Modes below the mid-range frequency show too much damping and those above show too little. [Ref. 7:p. 12]. Johnson and

Keinholz suggested multiplying the loss factor obtained in the described iterative method by $(G_i/G_{ref})^{1/2}$, where G_i is the viscoelastic material shear modulus at the i th natural frequency and G_{ref} is the core shear modulus at the mid-range frequency. Once the matrices of natural frequency, mode shape, strain energy fraction and loss factor were calculated for each plate, Equation (3.7) was solved and the frequency response amplitude was plotted as a function of frequency.

2. Frequency Response Method

Use of the NMSC/NASTRAN model frequency response analysis to directly calculate response amplitude within the finite element program requires the viscoelastic material properties to be input as constants throughout the frequency range analyzed. This restriction limits the modal frequency response analysis to frequency spans over which the viscoelastic materials shear modulus and loss factor have little change. Inspection of the nomogram in Figure 3.5 indicated a frequency span of no greater than 100 Hz would give little change in the viscoelastic material properties. In order to give the best accuracy at the peak response values, the natural frequencies of each plate were estimated by conducting a MSC/NASTRAN modal analysis using the mid-range viscoelastic material properties. The viscoelastic material shear modulus and loss factor were then obtained for the plate structures at each of these natural frequencies.

Modal frequency response analysis was then performed over 100 Hz spans centered at each natural frequency. The output magnitude versus frequency curves for each resonant frequency were compiled and plotted as composite curves. The modal frequency response analysis in MSC/NASTRAN for the simple plate is provided in Appendix B.

E. VIBRATION GENERATOR TESTING ARRANGEMENT

Experimentally determined vibration response analysis utilized a Wilcoxon research F3 vibration generator as the input force device. The F3 vibration generator was attached to the base plate on all applications. An HP 3562A Dynamic Signal Analyzer provided the swept sine driving signal which was amplified by a Wilcoxon research power amplifier (Model PA7C). A force transducer was located before the attachment port at the base of the vibration generator to measure the input excitation force. The force signal was amplified by a charge amplifier and fed as the input signal to the HP 3562A Dynamic Signal Analyzer. An Endevco accelerometer was placed at a symmetrically opposite point on each plate and coupled with a signal conditioner to provide the output signal to the HP 3562A Dynamic Signal Analyzer. Figures 3.6-3.8 show the locations of the vibration generator and accelerometer. The HP 3562A Dynamic Signal Analyzer converted the signals to digitized data and computed the frequency response, coherence and power spectra. Descriptive points were taken from the HP 3562A Dynamic

Signal Analyzer display of frequency response and plotted on the same graph as the finite element predictions.

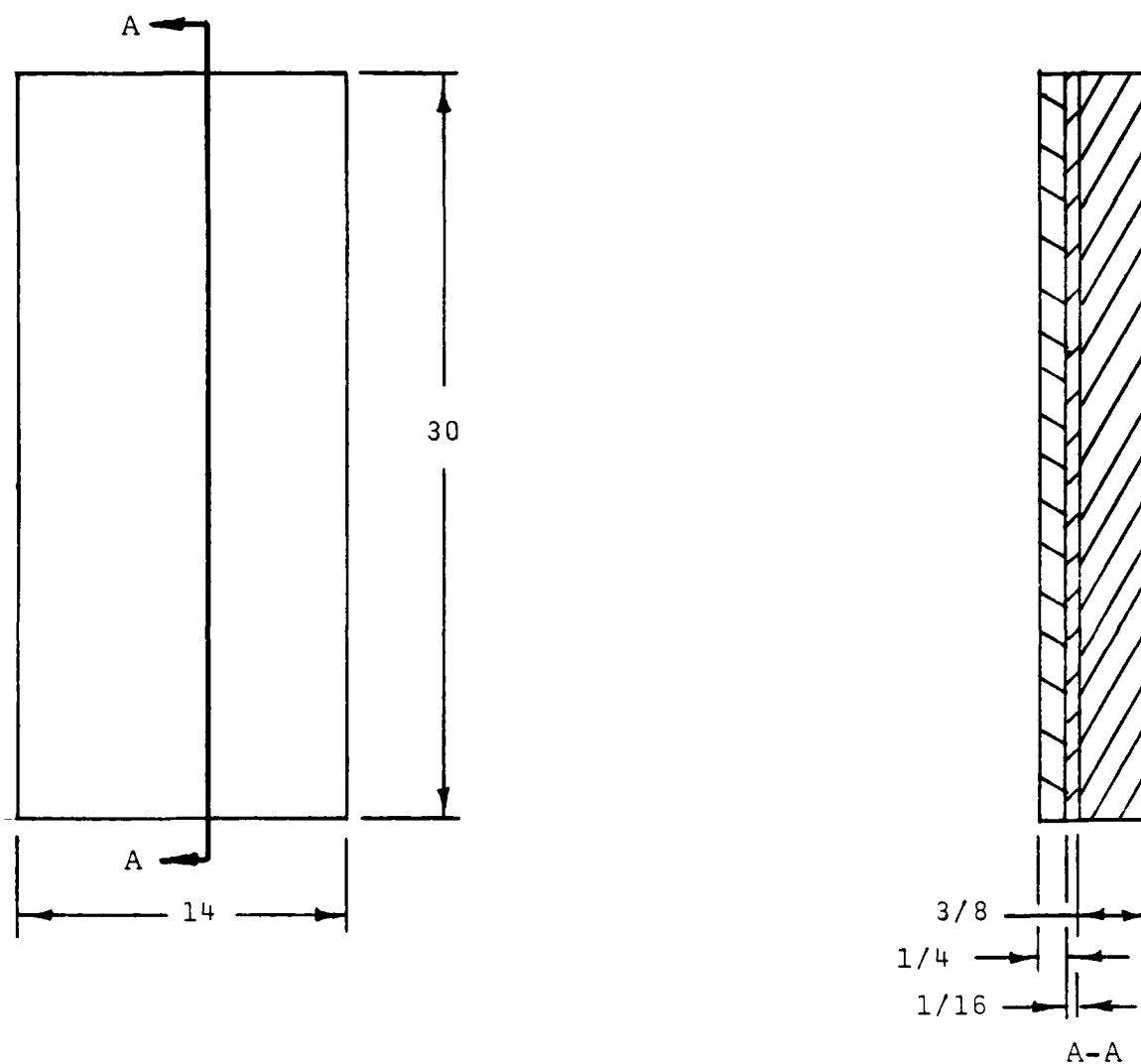


Figure 3.1 Dimensions of Simple Plate with Applied Viscoelastic and Constraining Layers

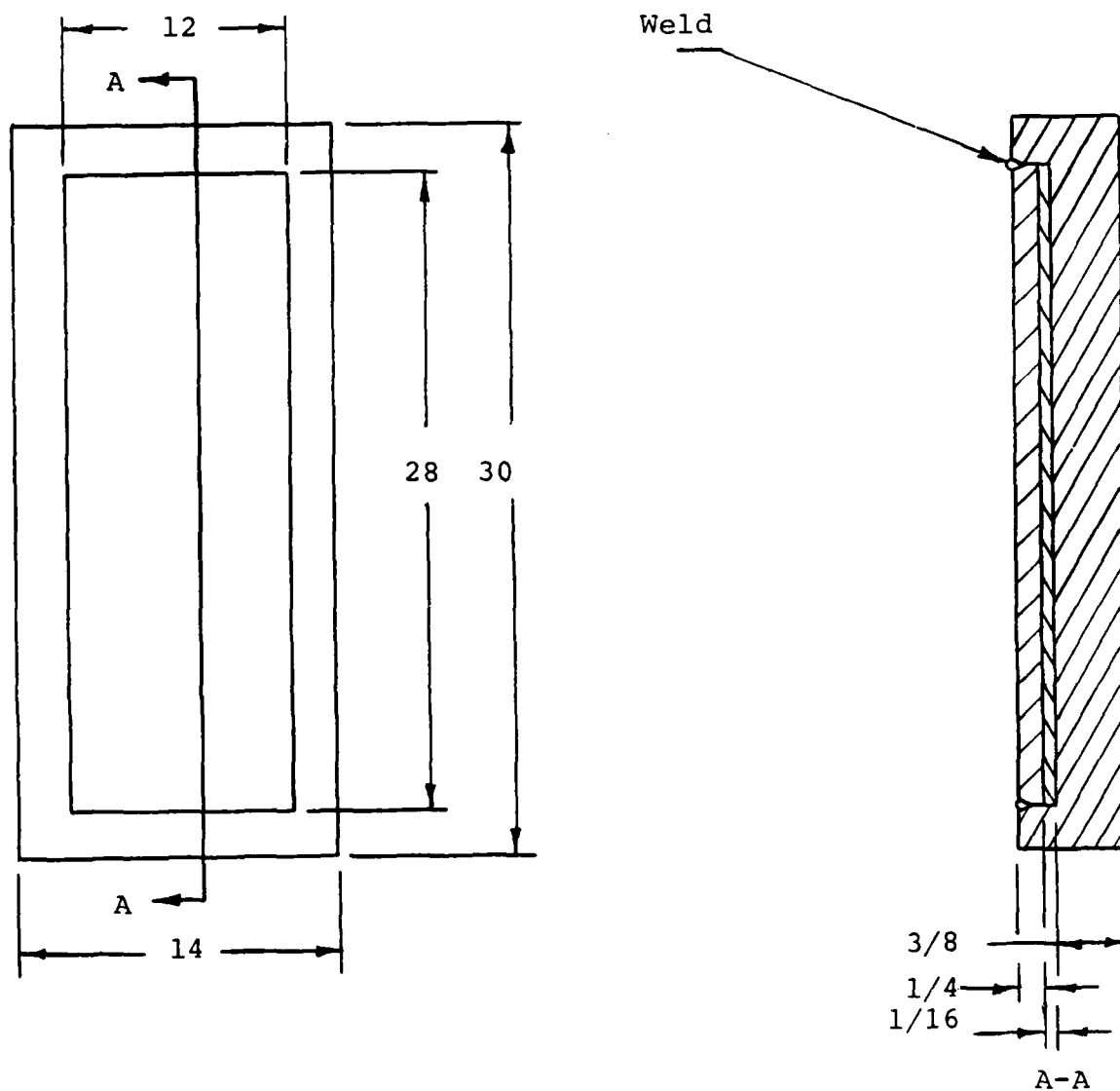


Figure 3.2 Dimensions of Milled Plate with Applied Viscoelastic and Constraining Layers

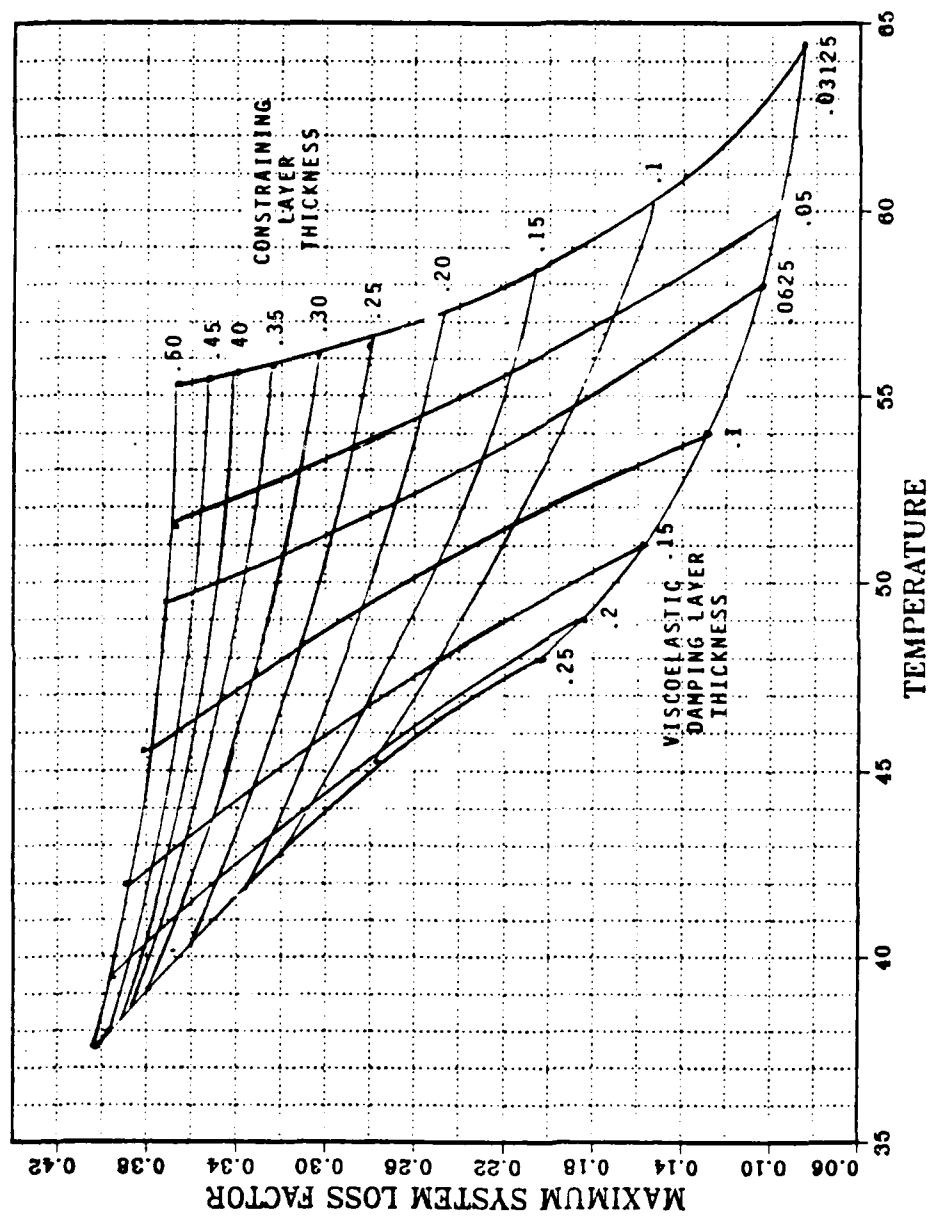


Figure 3.3 Estimate of System Loss Factor of the Simple Plate With Varying Thicknesses of Viscoelastic Damping and Constraining Layers

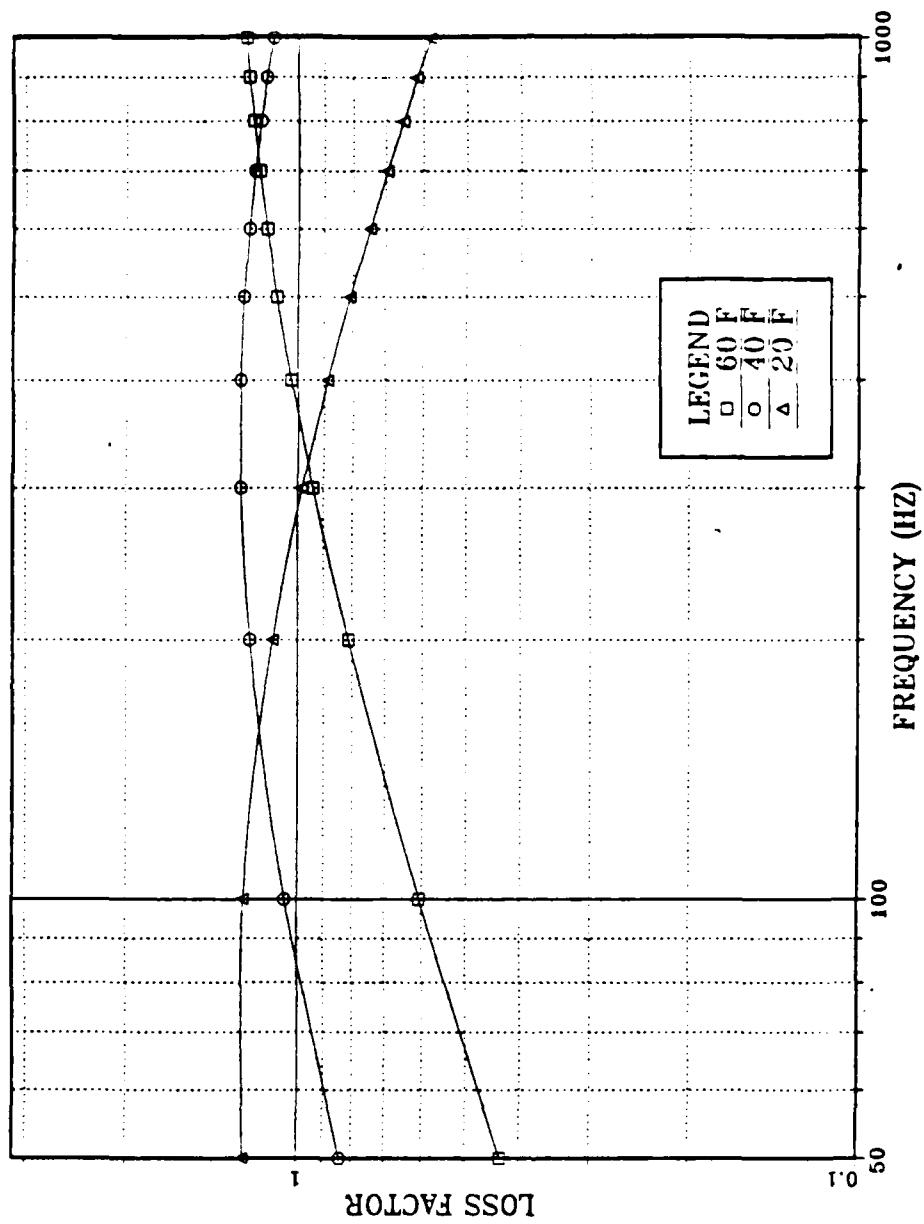


Figure 3.4 Loss Factor Variation of ISD-112 with Varying Frequency and Temperature

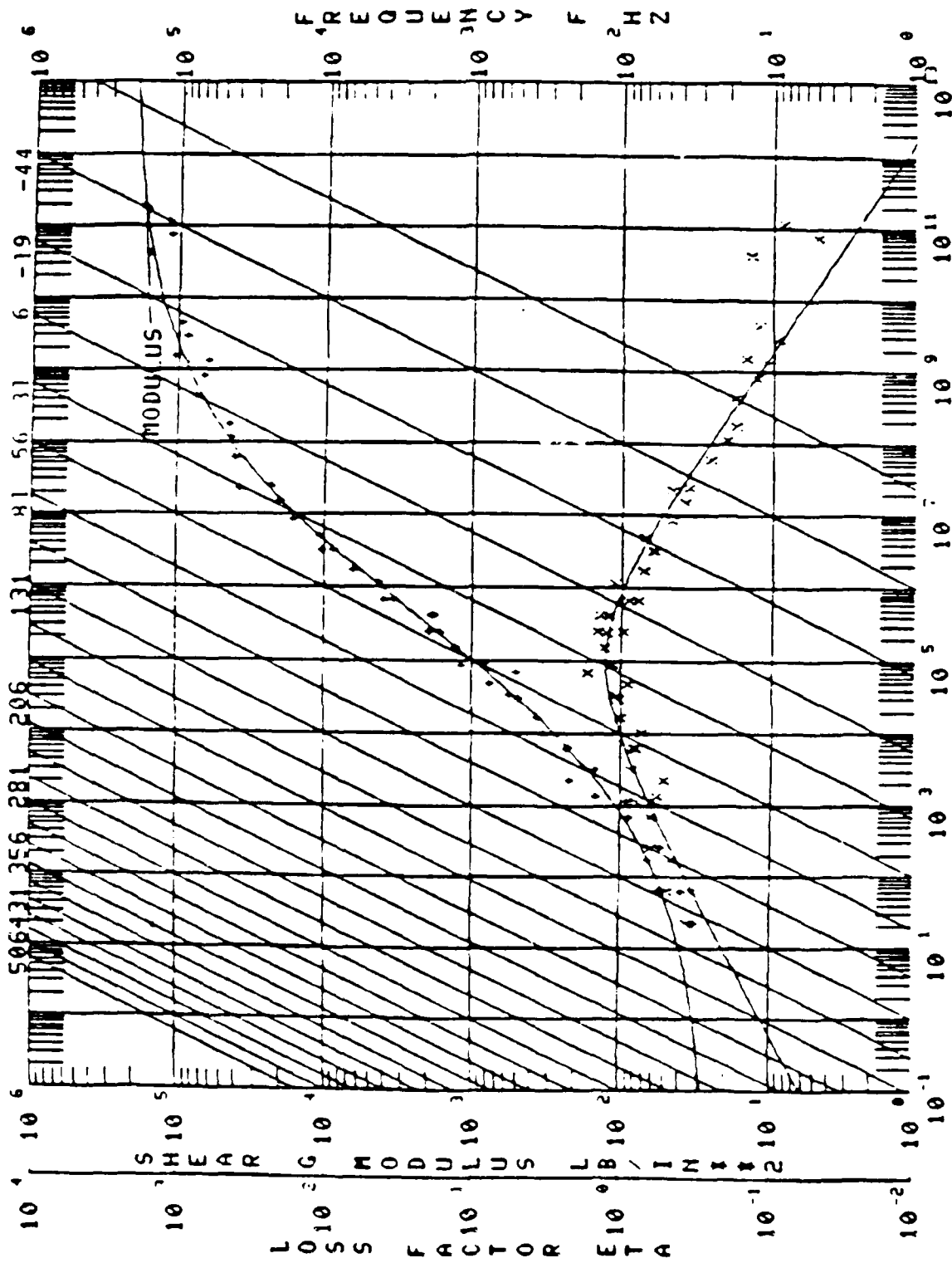


Figure 3.5 University of Dayton Nomogram for 3M ISD-112 Damping Material

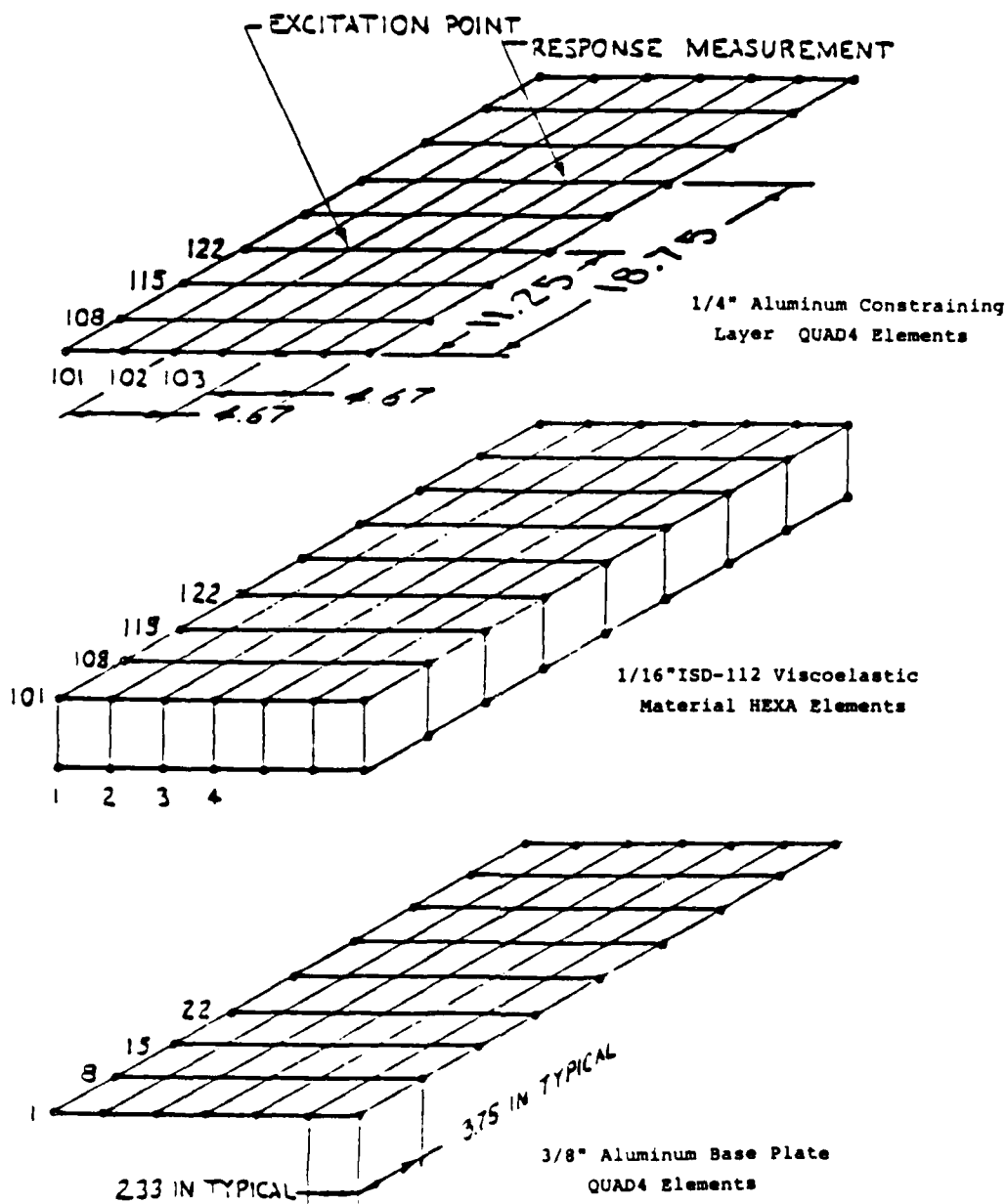


Figure 3.6 MSC/NASTRAN Finite Element Model for Simple Plate

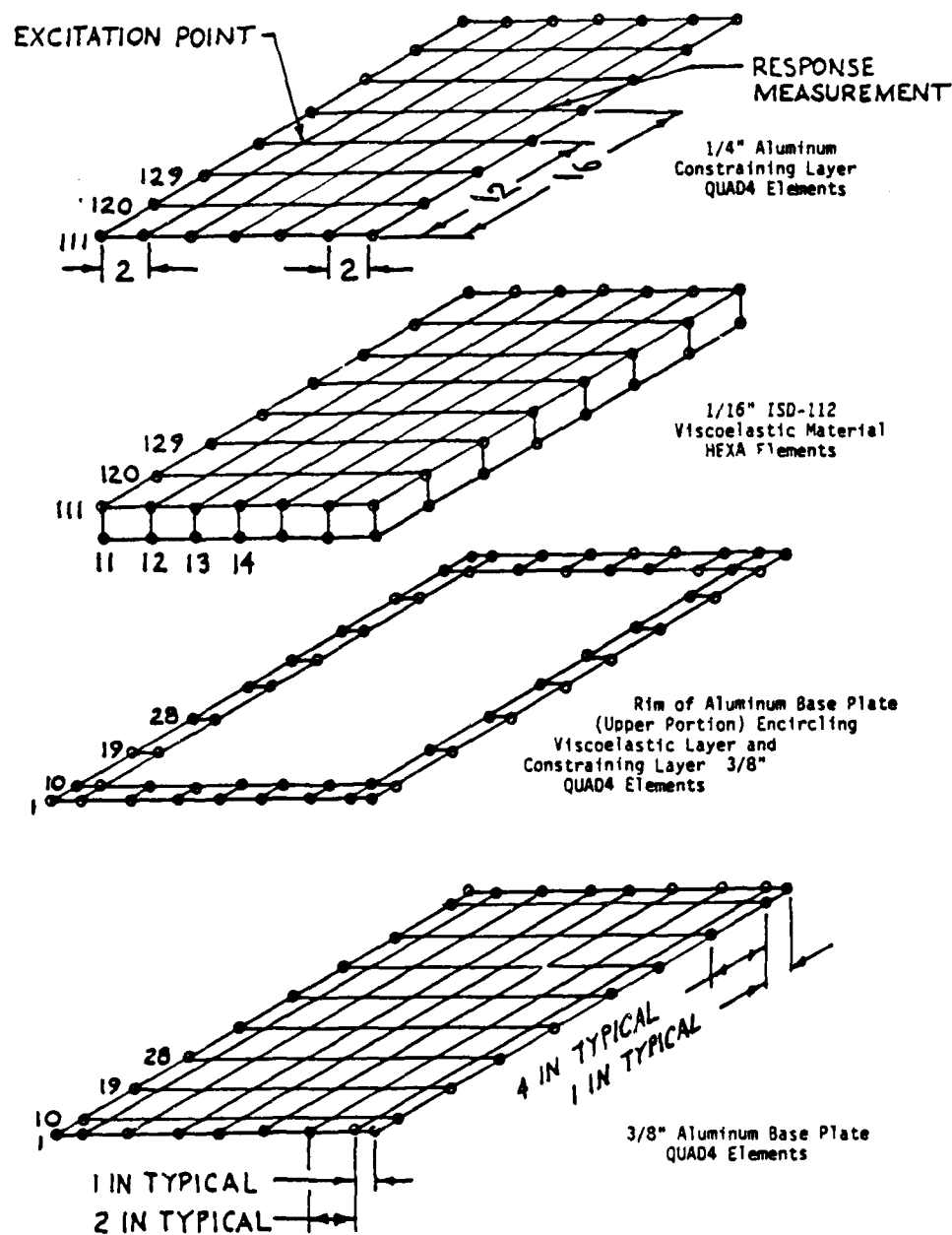


Figure 3.7 MSC/NASTRAN Finite Element Model for Milled Plate with Free Constraining Layer

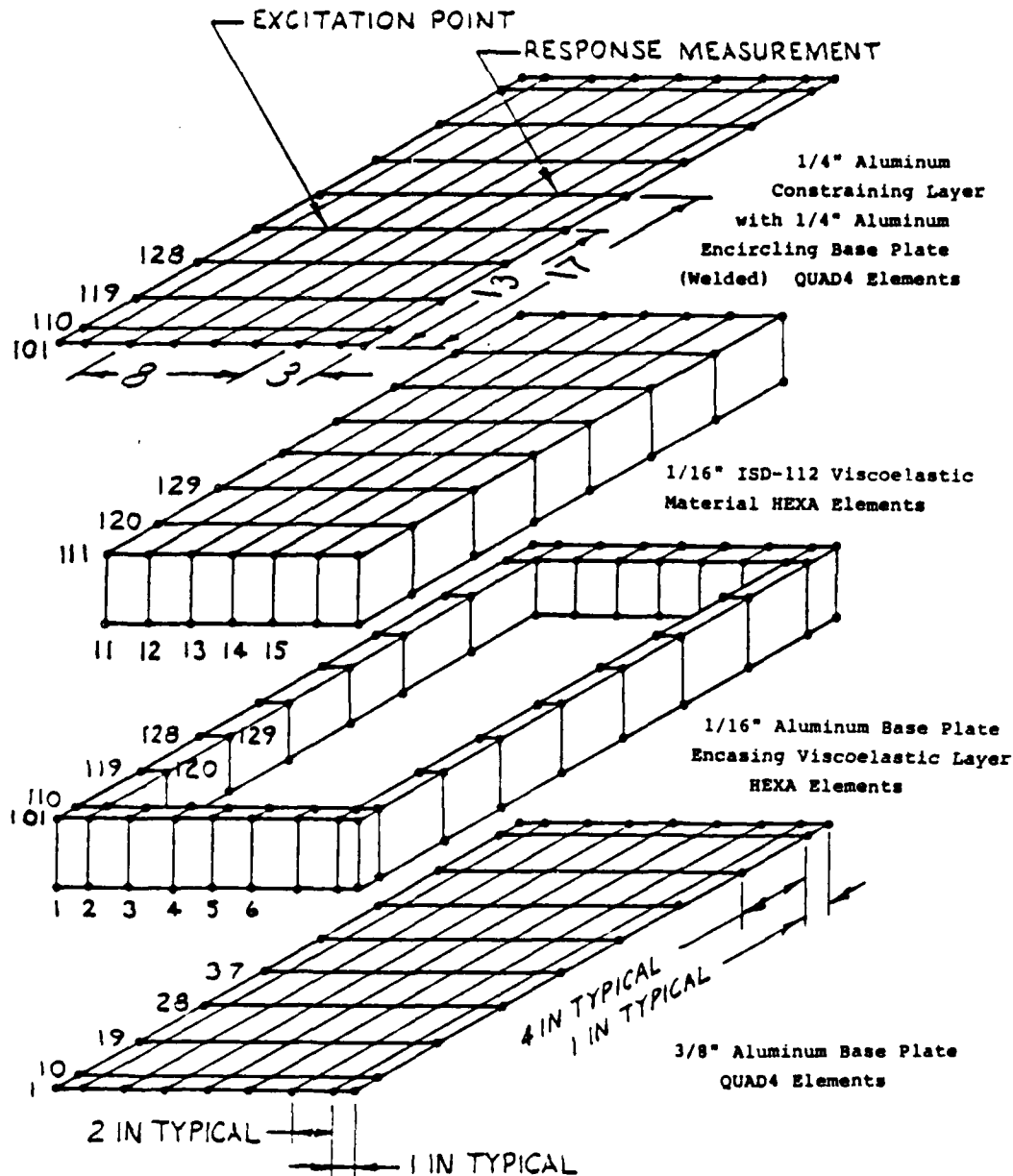


Figure 3.8 MSC/NASTRAN Finite Element Model for Milled Plate with Welded Constraining Layer

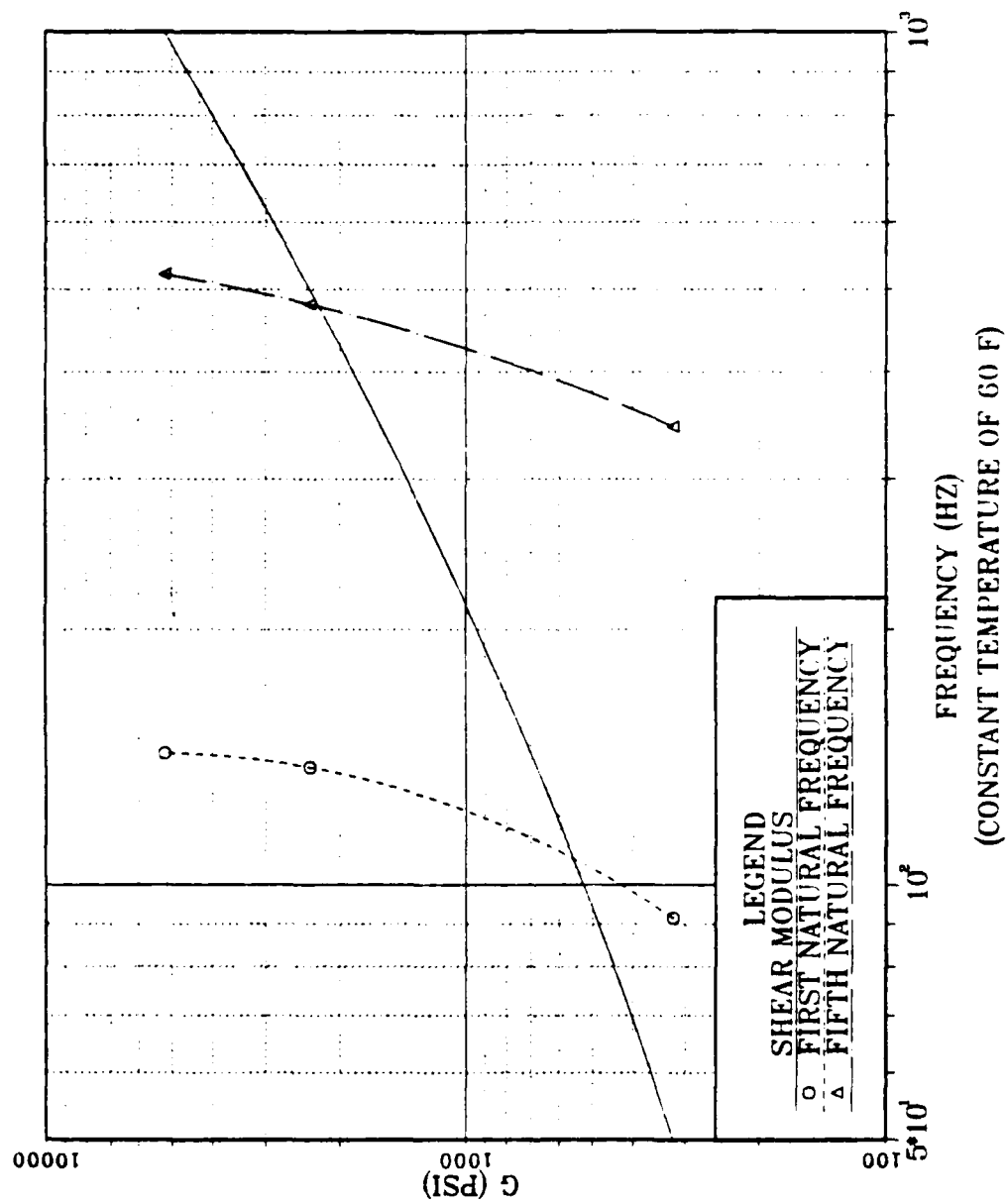


Figure 3.9 Iterative Method for the Simple Plate Modes

IV. RESULTS

A series of response amplitude versus frequency plots were constructed for each plate. The first set of figures (Figures. 4.1-4.3) plots the experimental data for each plate before and after the application of the viscoelastic damping and constraining layers. After completing the two prediction methods, the results were plotted (Figures 4.4-4.6) with the experimental analysis for the damped plates.

A. SIMPLE PLATE

The experimental frequency response plot of the simple plate (Figure 4.1) shows a large increase in damping when the viscoelastic and constraining layers are applied. All natural frequencies shift lower in frequency and in some cases amplitude peaks are combined into a single peak. The system loss factor for the first mode increased from 2.2% to 34% and the third mode increased from 1.6% to 14% after the application of the viscoelastic material and constraining layer.

Comparison of the two simple plate prediction methods with each other and the experimental results show several differences (Figure 4.4). The MSE curve resonant frequencies differ from the NASTRAN composite curve, with the MSE resonant frequencies being slightly higher than the NASTRAN composite curve at frequencies below 500 Hz and

slightly lower at frequencies above 500 Hz. The resonant frequencies of the experimental data are lower than either prediction method throughout the frequency range inspected. The experimental data response peak amplitudes are higher than either of the prediction curves. The response peak amplitudes of the MSE method have approximately the same value as the NASTRAN composite curve with the poorest matching above 600 Hz and the best matching at the first peak. The experimental data show a loss factor of 34% for the first mode while both prediction methods indicate a 45% loss factor. The third mode has a 14% loss factor for the experimental data and a 20% loss factor for the prediction methods.

B. MILLED PLATE, FREE CONSTRAINING LAYER

The experimental frequency response plot shows a large decrease in peak response amplitudes after the viscoelastic damping treatment (Figure 4.2). In several cases, multiple amplitude peaks are again combined into a single peak. The system loss factor in the 300 Hz range was 1% prior to damping. Application of the damping material increases the system loss factor to 4% in this range.

The prediction methods were plotted for the finite element model in Figure 4.5 with the two prediction methods showing good correlation. At frequencies below 500 Hz both prediction methods show similar peak response amplitudes but at differing frequencies with the NASTRAN composite method

having consistently lower peak frequencies. Above 500 Hz both prediction methods again show similar amplitudes but the MSE method showed lower peak frequencies. The prediction curves are poorly matched above 900 Hz. The experimental data show similar resonant frequencies but the frequency peaks are sharper than either prediction method over the observed frequency range. The experimental system loss factor at the 300 Hz peak is 4% while both prediction methods indicate a 6% loss factor.

C. MILLED PLATE WITH WELDED CONSTRAINING LAYER

After the experimental analysis of the unwelded milled plate, the plate constraining layer was welded to the base plate while maintaining the majority of the plate surfaces below 200° F during the welding process. After welding, the aluminum constraining layer and base plate were visibly warped and the plate resonated loudly when struck. The experimental analysis of the welded plate confirmed a significant decrease in damping (Figure 4.3). The experimental loss factors of the welded plate at all natural frequencies were indistinguishable from the experimental loss factors for the milled plate prior to the application of the viscoelastic layer. After the weld was cut, the plate once again exhibited high damping (Figure 4.7). The plot of the two finite element predictions (Figure 4.6) yielded curves matched for frequencies below 700 Hz and curves beginning to disagree above 700 Hz.

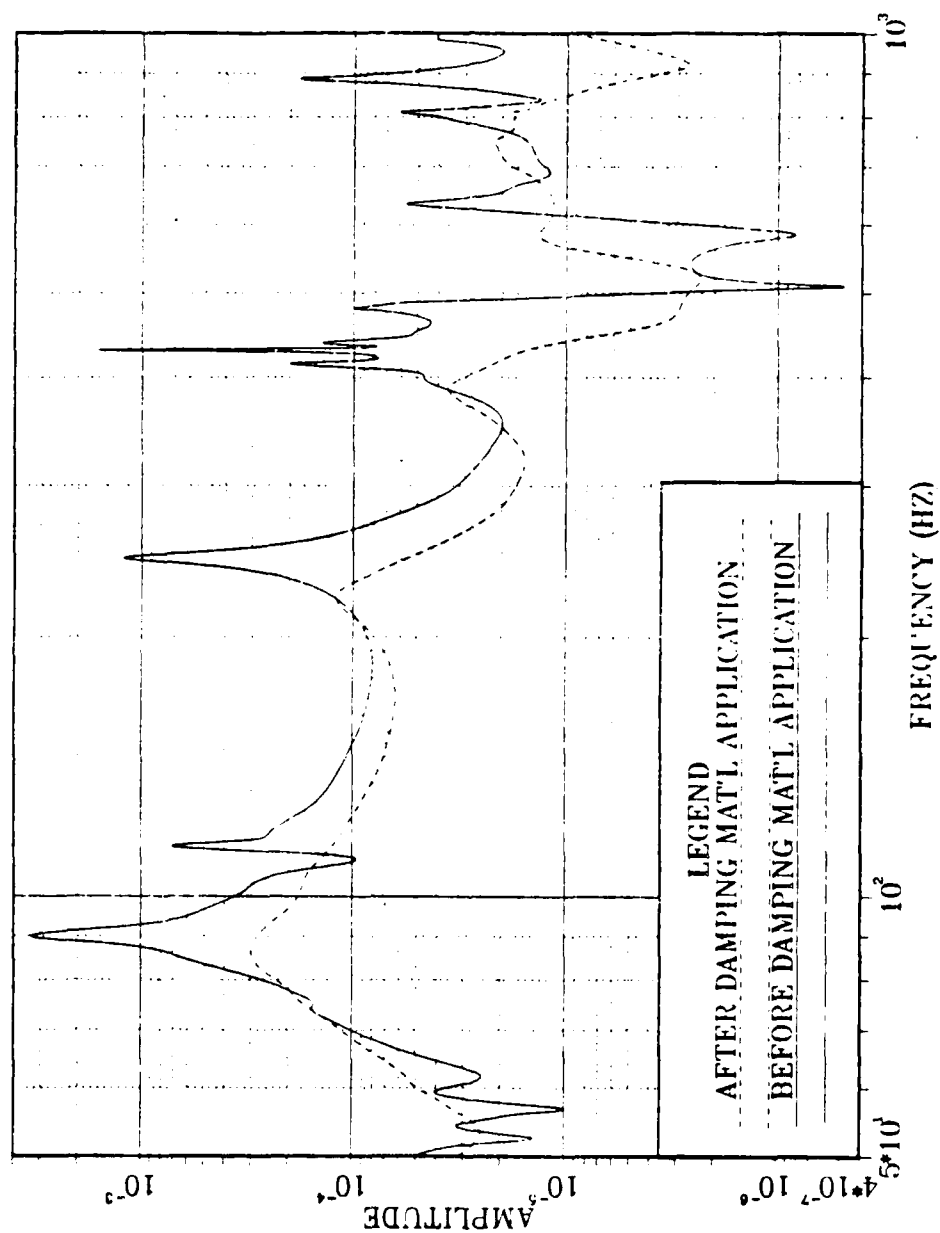


Figure 4.1 Simple Plate, Experimental Data Before and After Application of Viscoelastic Damping Treatment

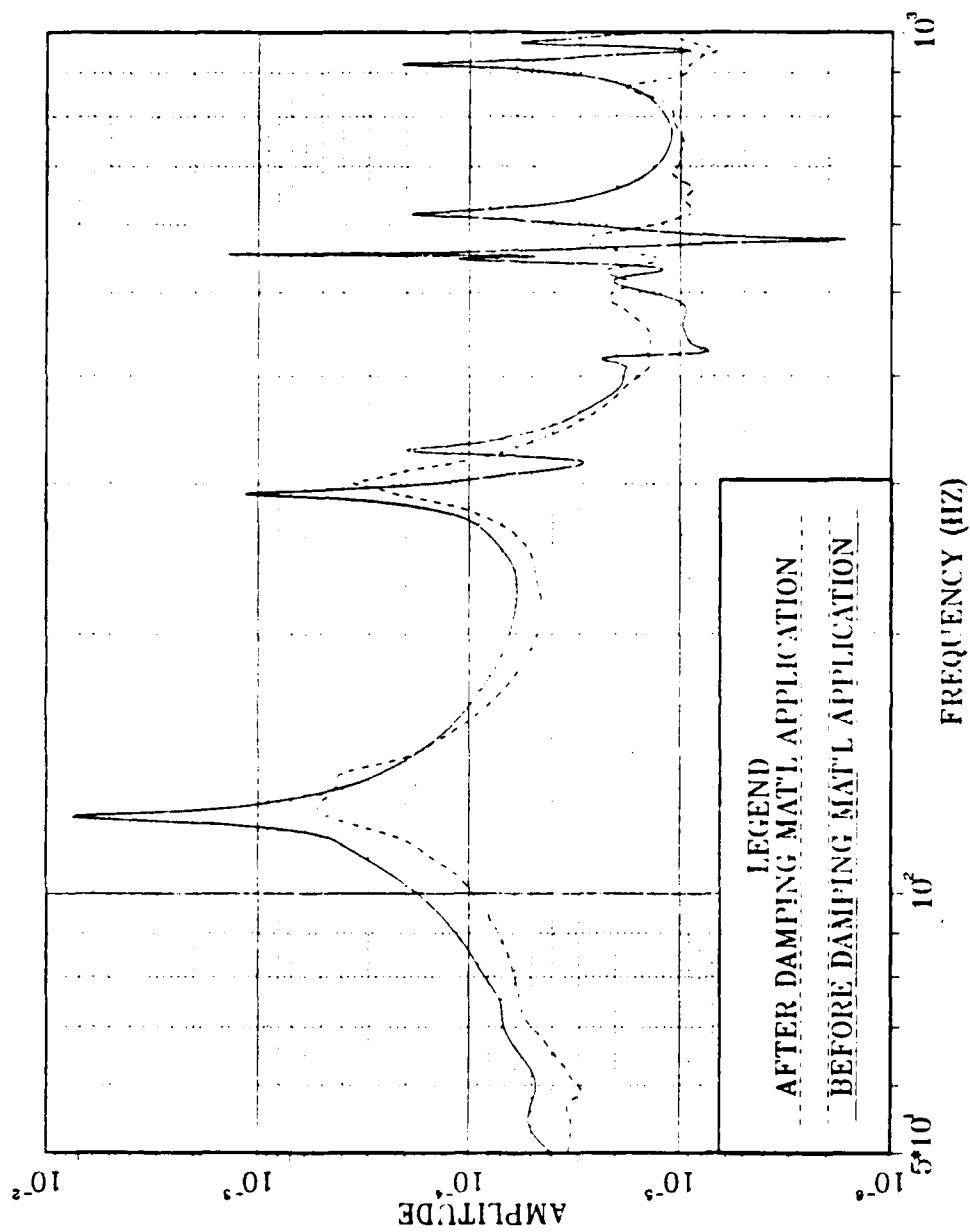


Figure 4.2 Milled Plate with Free Constraining Layer, Experimental Data Before and After Application of Viscoelastic Damping Treatment

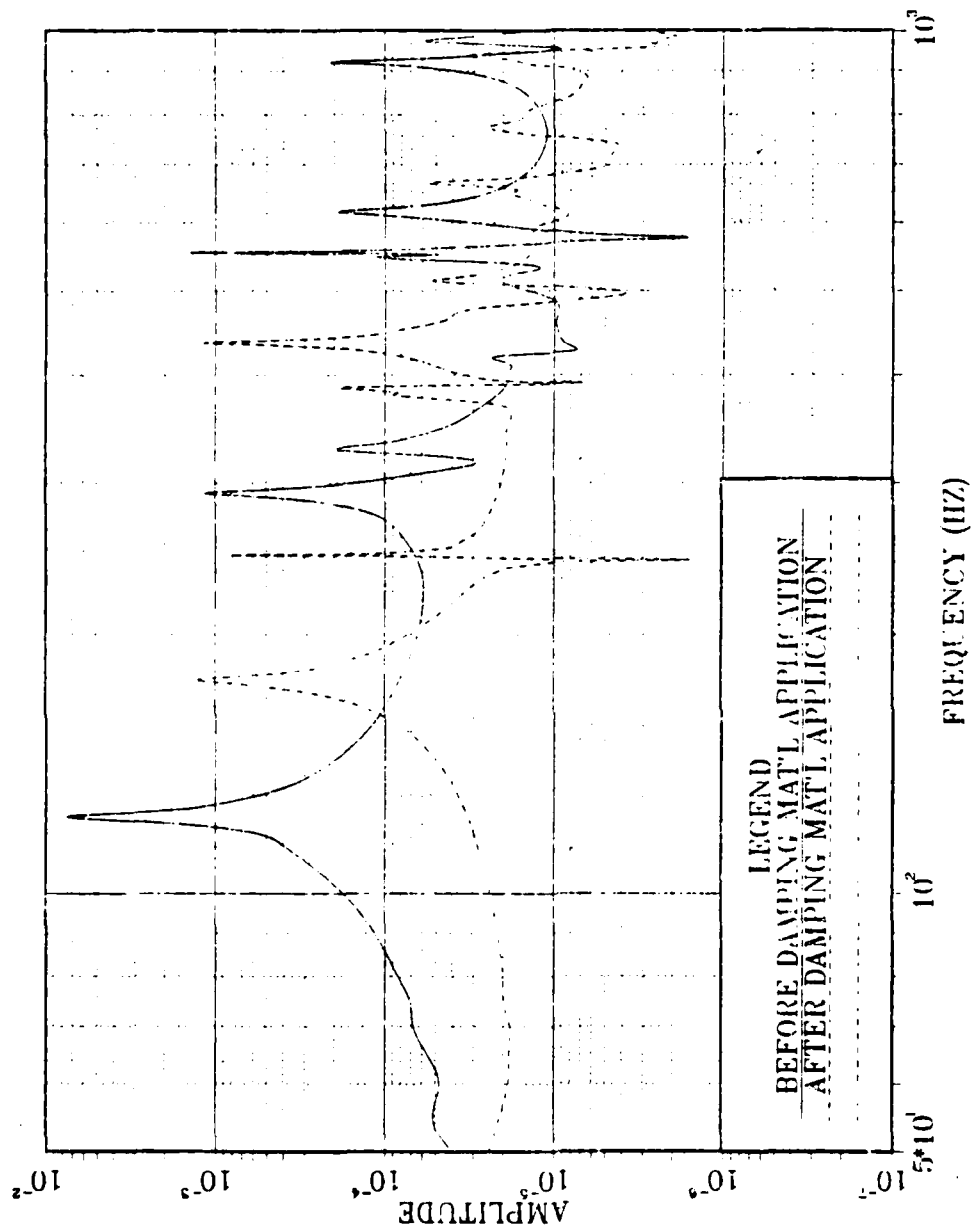


Figure 4.3 Welded Plate with Welded Constraining Layer, Experimental Data Before and After Application of Viscoelastic Damping Treatment

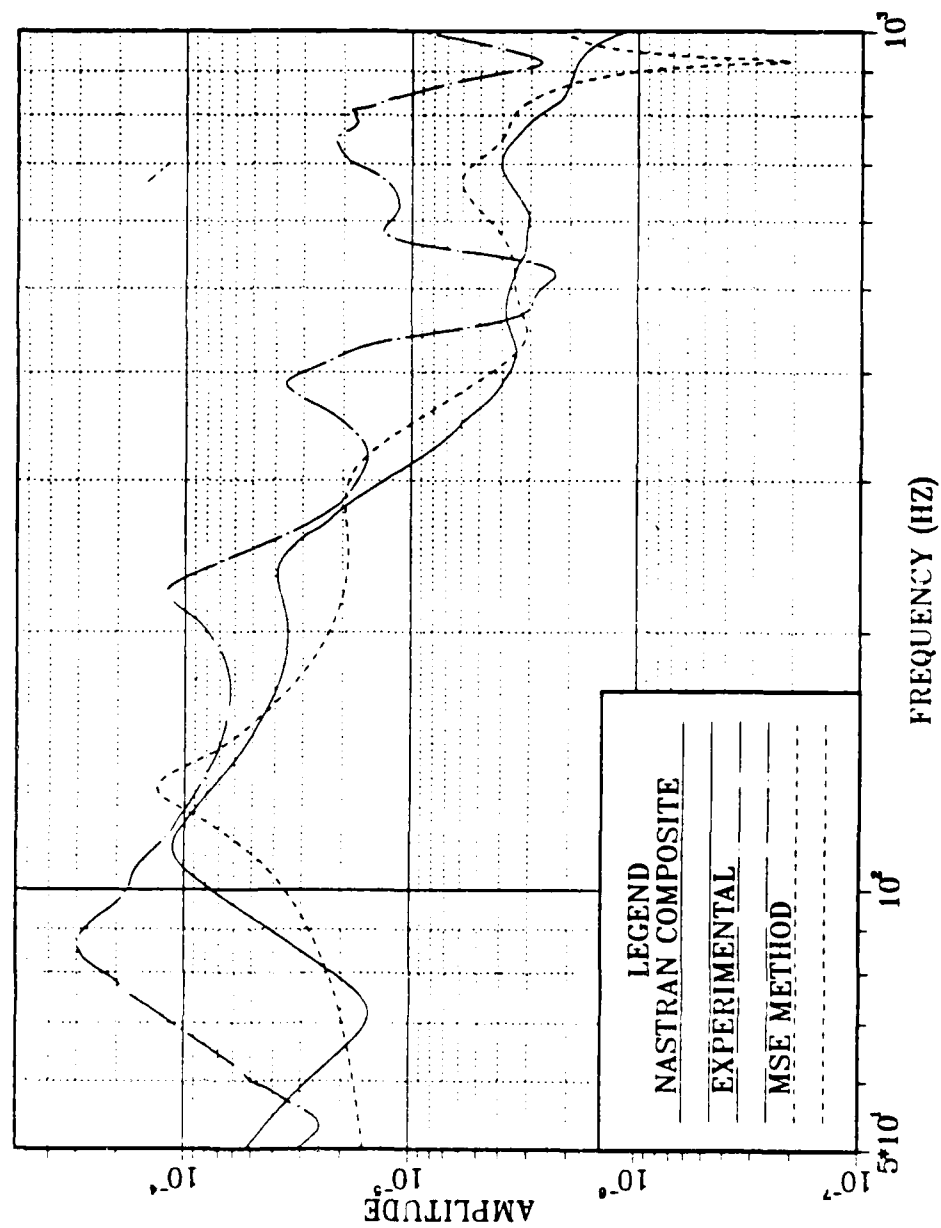


Figure 4.4 Simple Damped Plate, Experimental Data and Two Predictions Method Curves

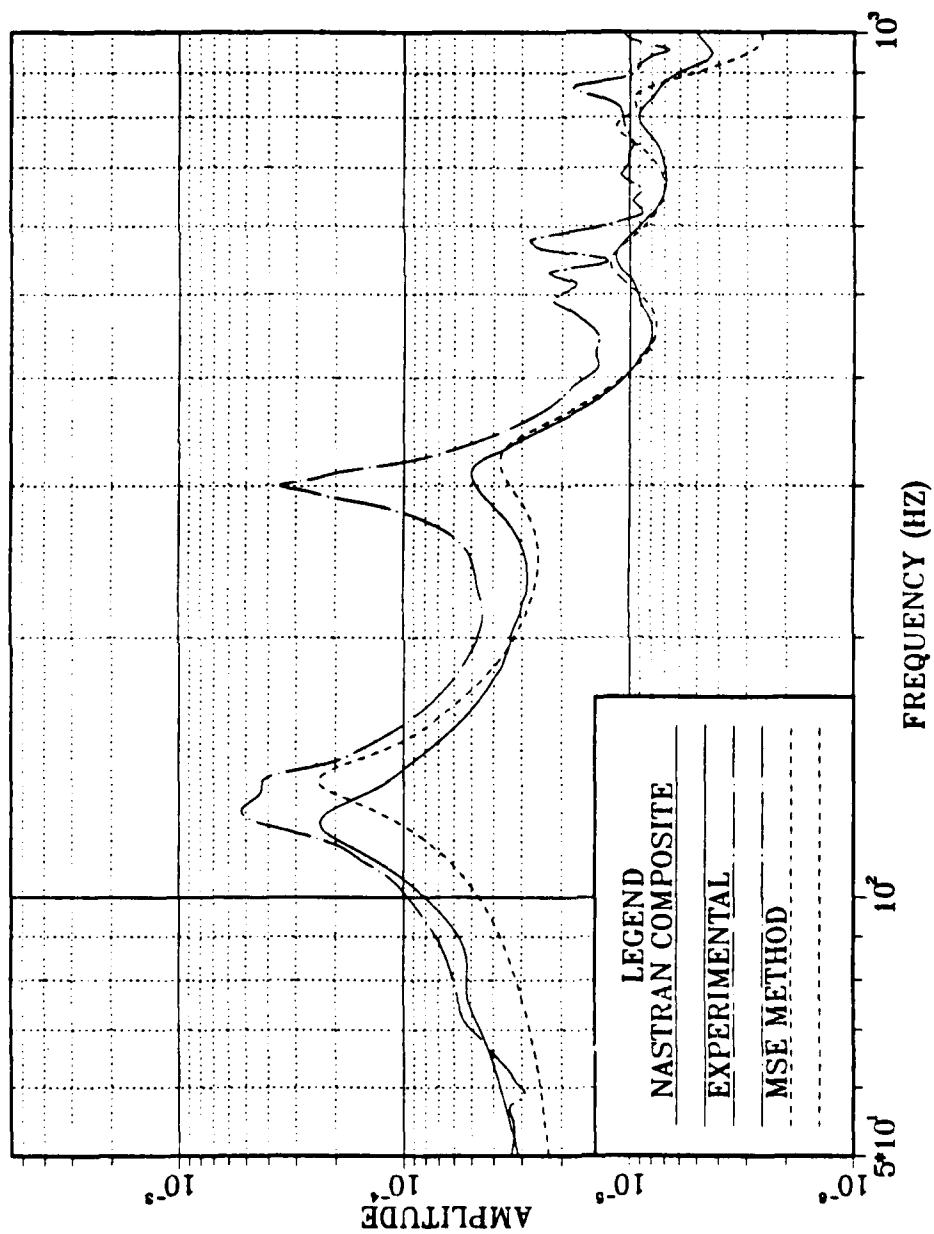


Figure 4.5 Milled Damped Plate with Free Constraining Layer,
Experimental Data and Two Predictions Method Curves

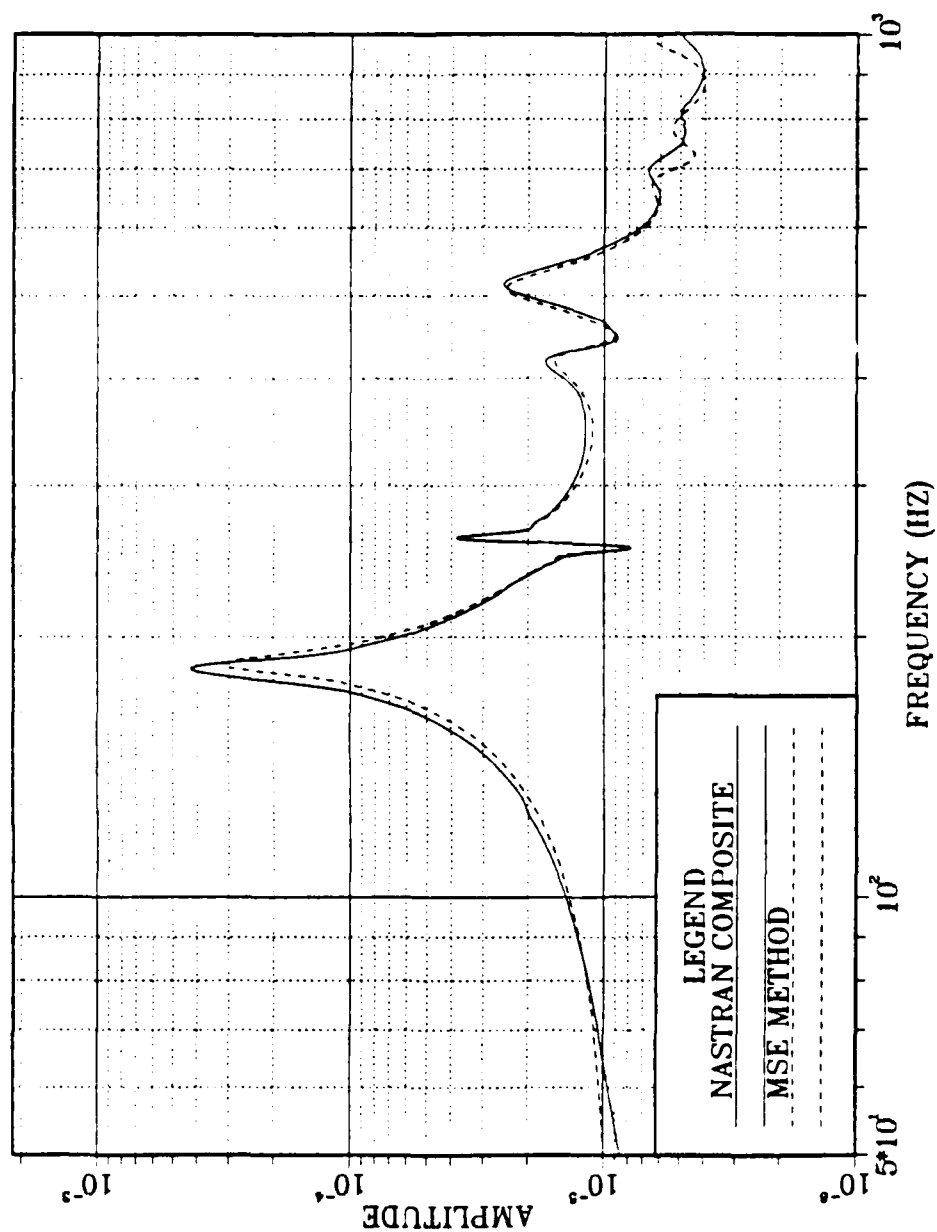


Figure 4.6 Milled Damped plate with Welded Constraining Layer, Two Predictions Method Curves

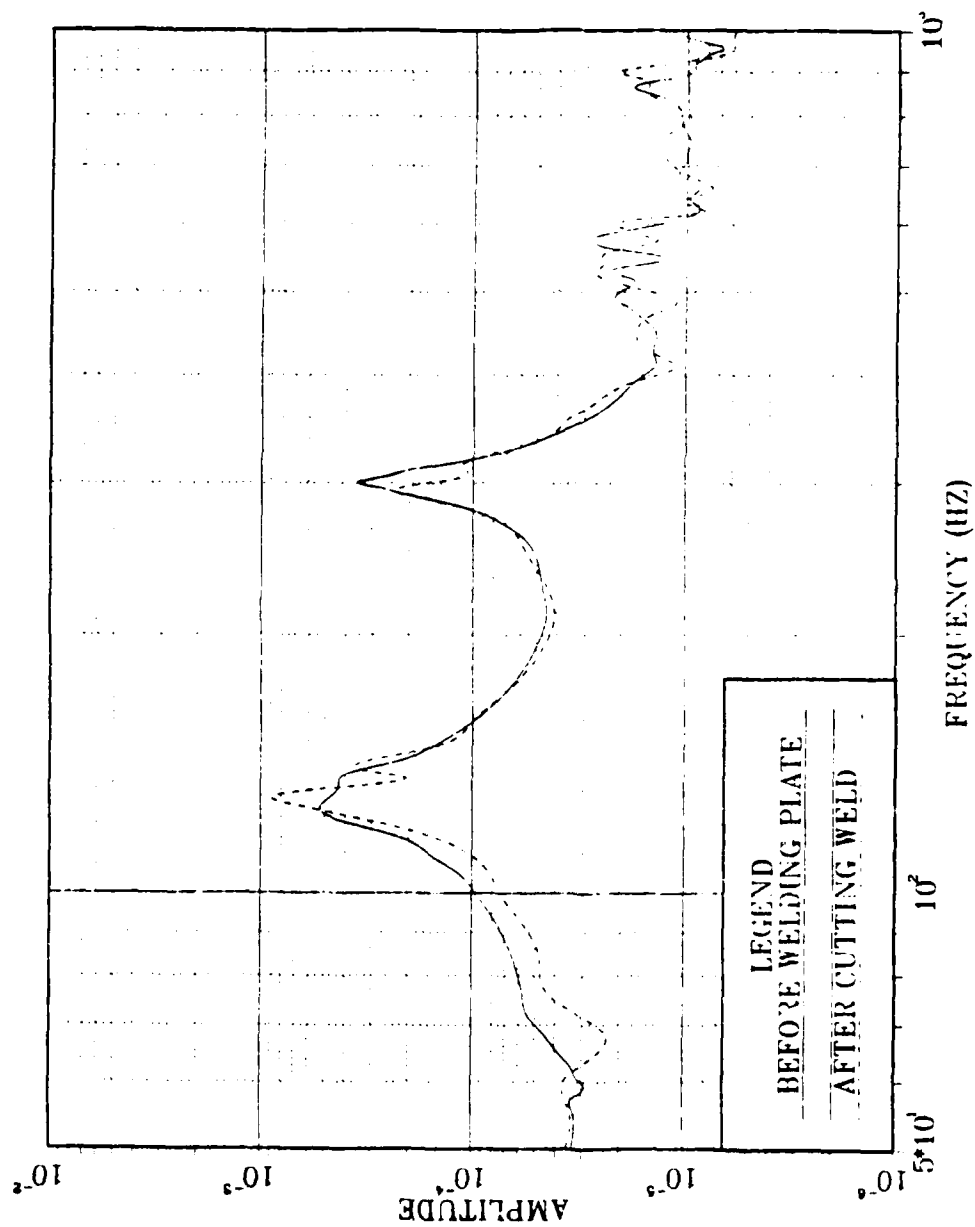


Figure 4.7 Milled Damped Plate Experimental Data Before Welding Constraining Layer and After Cutting Weld

V. CONCLUSIONS

Figure 4.1 shows the simple plate vibration response is reduced significantly after the 3M ISD-112 viscoelastic material and constraining layer are applied. Comparison of the experimental data and the two prediction methods in Figure 4.4, however, show that both the NASTRAN composite curve and the MSE method predict more damping than has occurred. Vibration energy absorbed by the viscoelastic layer is converted to heat and possibly increased the damping material temperature. No attempt to hold the plate temperature constant during the experimental analysis was made. Figure 3.9 shows that increasing the temperature of the viscoelastic material will decrease its loss factor. Another contributing factor to the lower actual damping may be the variation in the behavior of the viscoelastic material.

In examining the MSE method (Equation (3.7)), it can be seen that the off-resonant frequency terms have an increasing contribution to the predicted response amplitude as the frequency increases.

The natural frequencies of the MSE method are found using constant mid-range frequency viscoelastic material properties. This results in the MSE method amplitude peaks of Figure 4.4 shifting downward from the NASTRAN composite

curves in the high frequency range. An upward shift of the NASTRAN curves occurs in the low frequency range. The two prediction methods for the simple plate show more disagreement than for the other two plate models investigated. The MSE summation Equation (3.7) contained 18 modes for each plate analysis conducted. However the simple plate is the least stiff and thus 14 of these modes occur below 1000 Hz (78%). The milled plate had 10 modes below 1000 Hz before welding (56%) and 8 after welding (44%). The number of terms in the simple plate summation of Equation (3.8) should contain more terms to increase the accuracy of the MSE method prediction curve.

Inspection of the experimental analysis in Figure 4.2 again shows significant damping after application of the viscoelastic damping material and constraining layer. Figure 4.5 shows that both predicted damping levels were greater than the experimental data with the causes of the error being the same as for the simple plate. Examination of the two prediction curves shows the MSE method gives acceptable values of both amplitude and peak response frequency throughout the frequency range analyzed. The MSE prediction method of the milled plate with a free constraining layer again shows the MSE method response frequency shifts described in the simple plate MSE prediction.

After welding the constraining layer to the base plate, the structure was warped and exhibited no damping contributable to the viscoelastic material layer (Figure 4.6). When the weld was cut, the plate warpage decreased significantly and the milled plate once again displayed a large loss factor (Figure 4.7). This indicated that the viscoelastic layer had separated from the plates as a result of the warpage caused by the edge welding process. Because of the loss of damping through deformation of the plates during welding, only the two prediction methods for the milled plate with a welded constraining layer are plotted in Figure 4.6. This plate was the stiffest plate analyzed, having eight natural frequencies in the frequency range studied vice 10 natural frequencies for the milled plate prior to welding and 14 for the simple plate. As a result, the response amplitude of the MSE prediction method is in agreement with the NASTRAN composite prediction method. The MSE prediction method again shows a slight upward shift of the low frequency range peaks and a downward shift of the high range peaks.

Overall indications of the three plates show actual plate behavior is accurately estimated by both prediction methods. Errors occurring in the higher natural frequencies are due to an insufficient number of terms in the MSE summation Equation (3.4). Where inaccuracies occur, the MSE prediction method is found to be a good approximation of the

NASTRAN prediction method and should be an acceptable substitute for the NASTRAN composite prediction method. The simplicity of application coupled with the low computer time required make the MSE method the most attractive choice for engineering analysis which must consider both a wide range of environmental conditions and several design configurations.

VI. RECOMMENDATIONS

The following are suggestions for further studies in this field:

1. This study investigated prediction accuracies of the MSE and composite method at constant temperature. Accuracy over a temperature span should be investigated.
2. The results of the MSE method were heavily dependent on the MSC/NASTRAN normal mode analysis conducted with viscoelastic properties evaluated at 500 Hz. An investigation of the prediction sensitivity to shifts in evaluation frequency is recommended.
3. The use of the HEXA8 solid finite element to model the viscoelastic layer gives results in an MSC/NASTRAN program which requires significant computer time to solve. Use of the viscoelastic beam element to model the viscoelastic layer have been suggested to reduce computer time requirements. [Ref. 14:pp. 352-354]
4. Failure of the welded plates viscoelastic material was due to the high temperature gradient causing warpage, yet failure to cool the surfaces of the plate would have resulted in destruction of the damping material. Investigation of welding techniques is required to give practicality to the milled plate design used in this paper.
5. Application of several viscoelastic material and constraining layers have been used on structures in order to broaden the frequency range at which damping occurs. Applying the prediction methods investigated to such multiple damping layers should be researched.
6. Viscoelastic material properties may vary from batch to batch of the same material. The construction of a nomogram using samples of the batch applied to the structure should greatly increase prediction accuracies.

APPENDIX A

NOMOGRAM LOSS FACTOR AND SHEAR MODULUS CALCULATIONS

As explained in Section III.A, it is impractical to use nomogram chart values of loss factor and shear modulus in analyzing damping characteristics of systems containing viscoelastic materials. All calculations of shear modulus and loss factor in this paper were accomplished through use of the FORTRAN program listed in Figures A.1-A.4. Although this program is not complicated, use of the equations without computer assistance is extremely tedious due to the large number of terms. Note that page 4 of the program (Figure A.4) also gives the system loss factor based on the Bernoulli-Euler equations (3.2)-(3.3). Equations (3.2) and (3.3) require Young's Modulus and the shear modulus values in order to be solved and thus it is most convenient to include these calculations here.

```

A.....PROGRAM CONSTANT AS DEFINED BELOW
AI.....PROGRAM CONSTANT AS DEFINED BELOW
BI.....PROGRAM CONSTANT AS DEFINED BELOW
BII.....PROGRAM CONSTANT AS DEFINED BELOW
BL.....LENGTH OF BEAM USED TO APPROXIMATE PLATE
BW.....WIDTH OF BEAM USED TO APPROXIMATE PLATE
C.....PROGRAM CONSTANT AS DEFINED BELOW
CI.....PROGRAM CONSTANT AS DEFINED BELOW
D.....PROGRAM CONSTANT AS DEFINED BELOW
EI.....MODULUS OF ELASTICITY OF BASE PLATE
E3.....MODULUS OF ELASTICITY OF CONSTRAINING LAYER
ED.....MODULUS OF ELASTICITY OF VISCOELASTIC LAYER
ETA.....VISCOELASTIC MATERIAL LOSS FACTOR
ETAFOR..NOMOGRAM CUNSTANT (REF 5, PP. A4)
FRUL....NOMOGRAM CUNSTANT (REF 5, PP. A4)
FROM....NOMOGRAM CUNSTANT (REF 5, PP.A4)
F.....FREQUENCY AT WHICH SYSTEM IS ANALYZED
FR.....REDUCED FREQUENCY

```

Figure A.1 FORTRAN Program to Calculate the Viscoelastic Material Shear Modulus, Loss Factor and System Loss Factor (Page One)


```

G.....SHEAR MODULUS OF VISCOELASTIC MATERIAL (PSI)
H1.....THICKNESS OF BASE PLATE
H3.....THICKNESS OF CONSTRAINING LAYER
H0.....THICKNESS OF VISCOELASTIC LAYER
K.....PROGRAM CONSTANT AS DEFINED BELOW
L.....LENGTH OF PLATE ANALYZED
ML.....NOMOGRAM CONSTANT (REF 5, PP. A4)
MR0M.....NOMOGRAM CONSTANT (REF 5, PP. A4)
N.....NOMOGRAM CONSTANT (REF 5, PP. A4)
PR.....POISONS RATIO FOR THE BASE PLATE
        AND THE CONSTRAINING LAYER
SETA.....SYSTEM LOSS FACTOR
SH.....NOMOGRAM CONSTANT (REF 5, PP. A4)
SL.....NOMOGRAM CONSTANT (REF 5, PP.A4)
SP.....PROGRAM CONSTANT AS DEFINED BELOW
T.....TEMPERATURE AT WHICH SYSTEM IS ANALYZED
TZERO.....NOMOGRAM REF. TEMPERATURE (REF 5, PP. A4)
W.....WIDTH OF PLATE ANALYZED

```

Figure A.2 FORTRAN Program to Calculate the Viscoelastic Material Shear Modulus, Loss Factor and System Loss Factor (Page Two)

```

      REAL  A,A1,B,B1,BL,BW,C,C1,D,D1,E3,ED,ETAFRO,ETA,F,FROL,FROM,
      *G,H1,H3,HD,K,L,MRUM,ML,N,PR,SETA,SH,SL,SP,T,TZERO,W
      **
      ** THE VISCOELASTIC AND CONSTRAINING LAYER THICKNESSES ARE INPUT **
      ** **
      WRITE(6,*) 'INPUT THE DAMPING MATERIAL THICKNESS'
      WRITE(6,*) 'INPUT THE CONSTRAINING LAYER THICKNESS'
      READ(6,*) H3,HD
      **
      ** MATERIAL PROPERTIES OF PLATE AND APPROXIMATING BEAM ARE DEFINED **
      ** **
      E1=10**7
      E3=E1
      PR=.3
      L=30
      W=14
      BL=2
      BW=1
      H1=.375
      K=(3.1416*BL/L)**2*(3.1416*BW/W)**2
      **
      ** ENVIRONMENTAL CONDITIONS ARE DEFINED **
      ** **
      F=150.
      T=60.
      **
      ** ISD-112 VISCOELASTIC MATERIAL NOMOGRAM CONSTANTS ARE INPUT **
      ** **
      TZERO=131
      FROM=400000
      WROM=2059.5
      N=.270
      ML=28.427
      ETAFRO=1.25
      SL=.27
      SH=-.35
      FROL=150000
      C=1.3

```

Figure A.3 FORTRAN Program to Calculate the Viscoelastic Material Shear Modulus, Loss Factor and System Loss Factor (Page Three)

```

*****
* VISCOELASTIC MATERIAL SHEAR AND YOUNGS MODULUS ARE CALCULATED. *
*****
FR=10*((LOG10(F)-12*(T-TZERO))/(S25+T-TZERO))
G=10*((LOG10(ML)+(2*LOG10(MROM/ML))/(1+FROM/FR)*N)
ED=3*G
WRITE(6,*) 'SHEAR MODULUS OF DAMPING MATL=',G
WRITE(6,*) 'MODULUS OF DAMPING MATL=',ED
*****
* VISCOELASTIC MATERIAL LOSS FACTOR IS CALCULATED *
*****
A=(LOG10(FR)-LOG10(FROL))/C
B=SL+SH
D=SL-SH

ETA=10*((LOG10(ETAFRO)+A*B+D*(1-SQRT(1+A**2)))/(C/2))
WRITE(6,*) 'DAMPING MATERIAL LOSS FACTOR = ',ETA
*****
*****
SYSTEM LOSS FACTOR IS CALCULATED USING FOURTH ORDER BEAM THEORY *
*****
SP=G/(E3*H3*HD*K)
A1=3*E3/E1*H3/H1*(1+2*HD/H1+H3/H1)**2*SP
B1=C1*(1+E3/E1*H3**3)+A1*(1+SP*(1+ED/E1*HD/H1))*(1+ETA**2)
C1=(1+SP+SP*E3/E1*H3*H1)**2*(SP*ETA+SP*ETA*E3/E1*H3/H1)**2
SETA=A1/B1*ETA
WRITE(5,*) 'PLATE DAMPED LOSS FACTOR IS ',SETA

STOP
END

```

Figure A.4 FORTRAN Program to Calculate the Viscoelastic Material Shear Modulus, Loss Factor and System Loss Factor (Page Four)

APPENDIX B

MSC/NASTRAN CODE FOR SIMPLE PLATE NORMAL MODE ANALYSIS AND MSC/NASTRAN CODE FOR SIMPLE PLATE FREQUENCY RESPONSE ANALYSIS

While the MSC/NASTRAN code was used for all the finite element plates analyzed, listing each program would serve no useful purpose. For completeness, a normal mode analysis and a frequency response analysis are listed here for the simple plate structure (Figures B.1-B.10). The MSC/NASTRAN programs for the milled plate with free constraining layer and milled plate with welded constraining layer vary only in the geometric organization of the grid points and finite elements.

```

ID DYNAMICS,FREQ MOD
SOL 3
TIME 240
DIAG 8,9,13
CEND
TITLE=MODAL ANALYSIS 500 HZ PROPERTIES
ECHO=UNSORT
SPC=10
METHOD=1
ESE=ALL
DISP=ALL
OUTPUT(PLOT)
PLOTTER NASTRAN
PAPER SIZE 14. BY 10.
AXES=Z,X,Y
SET 1=ALL
FIND,SCALE,SET 1,ORIGIN 1
PLOT
PLOT MODAL DEFORMATION 0,1,THRU,15,SET 1,ORIGIN 1,SHAPE
BEGIN BULK
GRID,1,0,0,0,0
=,* (7),=,* (3.75),=
=7
GRID,2,0,2.3333,0,0
=,* (7),=,* (3.75),=
=7
GRID,3,0,4.6667,0,0
=,* (7),=,* (3.75),=
=7
GRID,4,0,7.,0,0
=,* (7),=,* (3.75),=
=7
GRID,5,0,9.3333,0,0
=,* (7),=,* (3.75),=
=7
GRID,6,0,11.6667,0,0
=,* (7),=,* (3.75),=
=7
GRID,7,0,14.,0,0
=,* (7),=,* (3.75),=
=7
GRID,101,0,0,0,.0625
=,* (7),=,* (3.75),=
=7

```

Figure B.1 MSC/NASTRAN Normal Mode Analysis of
the Simple Plate (Page One)

```

GRID,102,0,2.3333,0,.0625
=,* (7),=,* (3.75),=
=7
GRID,103,0,4.6667,0,.0625
=,* (7),=,* (3.75),=
=7
GRID,104,0,7.,0,.0625
=,* (7),=,* (3.75),=
=7
GRID,105,0,9.3333,0,.0625
=,* (7),=,* (3.75),=
=7
GRID,106,0,11.6667,0,.0625
=,* (7),=,* (3.75),=
=7
GRID,107,0,14.,0,.0625

```

```

=,* (7),=,* (3.75),=
=7
CQUAD4,1,100,1,2,9,8,,-.1875
=,* (6),=,* (7),* (7),* (7),* (7),,=
=6
CQUAD4,2,100,2,3,10,9,,-.1875
=,* (6),=,* (7),* (7),* (7),* (7),,=
=6
CQUAD4,3,100,3,4,11,10,,-.1875
=,* (6),=,* (7),* (7),* (7),* (7),,=
=6
CQUAD4,4,100,4,5,12,11,,-.1875
=,* (6),=,* (7),* (7),* (7),* (7),,=
=6
CQUAD4,5,100,5,6,13,12,,-.1875
=,* (6),=,* (7),* (7),* (7),* (7),,=
=6
CQUAD4,6,100,6,7,14,13,,-.1875
=,* (6),=,* (7),* (7),* (7),* (7),,=
=6
CQUAD4,101,101,101,102,109,108,,.125
=,* (6),=,* (7),* (7),* (7),* (7),,=
=6
CQUAD4,102,101,102,103,110,109,,.125
=,* (6),=,* (7),* (7),* (7),* (7),,=
=6

```

Figure B.2 MSC/NASTRAN Normal Mode Analysis of the Simple Plate (Page Two)

```

C3UAD4,103,101,103,104,111,110,,.125
=,* (6),=,* (7),* (7),* (7),* (7),,=
=5
C3UAD4,104,101,104,105,112,111,,.125
=,* (6),=,* (7),* (7),* (7),* (7),,=
=5
C3UAD4,105,101,105,106,113,112,,.125
=,* (6),=,* (7),* (7),* (7),* (7),,=
=6
C3UAD4,106,101,106,107,114,113,,.125
=,* (6),=,* (7),* (7),* (7),* (7),,=
=6
CHEXA,201,200,1,2,9,8,101,102,+01
=,* (6),=,* (7),* (7),* (7),* (7),* (7),* (7),* (1)
=,* (6),=,* (7),* (7),* (7),* (7),* (7),* (7),* (1)
=,* (6),=,* (7),* (7),* (7),* (7),* (7),* (7),* (1)
=,* (6),=,* (7),* (7),* (7),* (7),* (7),* (7),* (1)
=,* (6),=,* (7),* (7),* (7),* (7),* (7),* (7),* (1)
=,* (6),=,* (7),* (7),* (7),* (7),* (7),* (7),* (1)
=,* (6),=,* (7),* (7),* (7),* (7),* (7),* (7),* (1)
+01,109,108
*1,*7,*7
*1,*7,*7
*1,*7,*7
*1,*7,*7
*1,*7,*7
*1,*7,*7
*1,*7,*7
CHEXA,202,200,2,3,10,9,102,103,+09
=,* (6),=,* (7),* (7),* (7),* (7),* (7),* (7),* (1)
=,* (6),=,* (7),* (7),* (7),* (7),* (7),* (7),* (1)
=,* (6),=,* (7),* (7),* (7),* (7),* (7),* (7),* (1)
=,* (6),=,* (7),* (7),* (7),* (7),* (7),* (7),* (1)
=,* (6),=,* (7),* (7),* (7),* (7),* (7),* (7),* (1)
=,* (6),=,* (7),* (7),* (7),* (7),* (7),* (7),* (1)
=,* (6),=,* (7),* (7),* (7),* (7),* (7),* (7),* (1)
+09,110,109
*1,*7,*7
*1,*7,*7
*1,*7,*7
*1,*7,*7
*1,*7,*7

```

Figure B.3 MSC/NASTRAN Normal Mode Analysis of
the Simple Plate (Page Three)

```

*1,*7,*7
*1,*7,*7
CHEXA,203,200,3,4,11,10,103,104,+17
=,*(6),=,*(7),*(7),*(7),*(7),*(7),*(7),*(7),*(1)
=,*(6),=,*(7),*(7),*(7),*(7),*(7),*(7),*(7),*(1)
=,*(6),=,*(7),*(7),*(7),*(7),*(7),*(7),*(7),*(1)
=,*(6),=,*(7),*(7),*(7),*(7),*(7),*(7),*(7),*(1)
=,*(6),=,*(7),*(7),*(7),*(7),*(7),*(7),*(7),*(1)
=,*(6),=,*(7),*(7),*(7),*(7),*(7),*(7),*(7),*(1)
=,*(6),=,*(7),*(7),*(7),*(7),*(7),*(7),*(7),*(1)
+17,111,110
*1,*7,*7
*1,*7,*7
*1,*7,*7
*1,*7,*7
*1,*7,*7
*1,*7,*7
*1,*7,*7
CHEXA,204,200,4,5,12,11,104,105,+25
=,*(6),=,*(7),*(7),*(7),*(7),*(7),*(7),*(7),*(1)
=,*(6),=,*(7),*(7),*(7),*(7),*(7),*(7),*(7),*(1)
=,*(6),=,*(7),*(7),*(7),*(7),*(7),*(7),*(7),*(1)
=,*(6),=,*(7),*(7),*(7),*(7),*(7),*(7),*(7),*(1)
=,*(6),=,*(7),*(7),*(7),*(7),*(7),*(7),*(7),*(1)
=,*(6),=,*(7),*(7),*(7),*(7),*(7),*(7),*(7),*(1)
=,*(6),=,*(7),*(7),*(7),*(7),*(7),*(7),*(7),*(1)
+25,112,111
*1,*7,*7
*1,*7,*7
*1,*7,*7
*1,*7,*7
*1,*7,*7
*1,*7,*7
*1,*7,*7
CHEXA,205,200,5,6,13,12,105,106,+33
=,*(6),=,*(7),*(7),*(7),*(7),*(7),*(7),*(7),*(1)
=,*(6),=,*(7),*(7),*(7),*(7),*(7),*(7),*(7),*(1)
=,*(6),=,*(7),*(7),*(7),*(7),*(7),*(7),*(7),*(1)
=,*(6),=,*(7),*(7),*(7),*(7),*(7),*(7),*(7),*(1)
=,*(6),=,*(7),*(7),*(7),*(7),*(7),*(7),*(7),*(1)
=,*(6),=,*(7),*(7),*(7),*(7),*(7),*(7),*(7),*(1)
=,*(6),=,*(7),*(7),*(7),*(7),*(7),*(7),*(7),*(1)
+33,113,112
*1,*7,*7
*1,*7,*7
*1,*7,*7
*1,*7,*7
*1,*7,*7

```

Figure B.4 MSC/NASTRAN Normal Mode Analysis of
the Simple Plate (Page Four)


```

*1,*7,*7
*1,*7,*7
CHEXA,206,200,6,7,14,13,106,107,+41
=,*(6),=,*(7),*(7),*(7),*(7),*(7),*(7),*(7),*(1)

```

```

=,*(6),=,*(7),*(7),*(7),*(7),*(7),*(7),*(7),*(1)
=,*(6),=,*(7),*(7),*(7),*(7),*(7),*(7),*(7),*(1)
=,*(6),=,*(7),*(7),*(7),*(7),*(7),*(7),*(7),*(1)
=,*(6),=,*(7),*(7),*(7),*(7),*(7),*(7),*(7),*(1)
=,*(6),=,*(7),*(7),*(7),*(7),*(7),*(7),*(7),*(1)
=,*(6),=,*(7),*(7),*(7),*(7),*(7),*(7),*(7),*(1)
+41,114,113
*1,*7,*7
*1,*7,*7
*1,*7,*7
*1,*7,*7
*1,*7,*7
*1,*7,*7
*1,*7,*7
PSHELL,100,100,.375,100
PSHELL,101,100,.25,100
PSOLID,200,200,0
MAT1,100,1.+7,.,.33,.,0955
MAT1,200,.,2354.02,.,49,.,035,.,1.089
PARAM,ASING,1
PARAM,AUTOSPC,YES
SPC1,10,6,101,THRU,163
SPC1,10,6,1,THRU,63
SUPPORT,32,12345
EIGR,1,MGIV,1.,1500.,.,24,.,.,+ZZ
+ZZ,MASS
PARAM,NTMASS,.,00259
ENDDATA

```

Figure B.5 MSC/NASTRAN Normal Mode Analysis of the Simple Plate (Page Five)

```

ID DYNAMICS,FREQ MOD
SOL 30
TIME 240
CEND
TITLE=FREQUENCY RESPONSE 500 HZ PROPERTIES
ECHO=UNSORT
SPC=10
METHOD=1
SVECTOR=ALL
DLOAD=2000
FREQUENCY=2100
SET 111=24
DISPLACEMENT(PHASE)=111
BEGIN BULK
GRID,1,0,0,0,0
=,* (7),=,* (3.75),=
=7
GRID,2,0,2.3333,0,0
=,* (7),=,* (3.75),=
=7
GRID,3,0,4.6667,0,0
=,* (7),=,* (3.75),=
=7
GRID,4,0,7.,0,0
=,* (7),=,* (3.75),=
=7
GRID,5,0,9.3333,0,0
=,* (7),=,* (3.75),=
=7
GRID,6,0,11.6667,0,0
=,* (7),=,* (3.75),=
=7
GRID,7,0,14.,0,0
=,* (7),=,* (3.75),=
=7
GRID,101,0,0,0,.0625
=,* (7),=,* (3.75),=
=7
GRID,102,0,2.3333,0,.0625
=,* (7),=,* (3.75),=
=7
GRID,103,0,4.6667,0,.0625
=,* (7),=,* (3.75),=
=7

```

Figure B.6 MSC/NASTRAN Frequency Response Analysis
of the Simple Plate (Page One)

```

GRID,104,0,7,,0,,.0625
=,* (7),=,=,* (3.75),=
=7
GRID,105,0,9.3333,0,,.0625
=,* (7),=,=,* (3.75),=
=7
GRID,106,0,11.6667,0,,.0625
=,* (7),=,=,* (3.75),=
=7
GRID,107,0,14,,0,,.0625
=,* (7),=,=,* (3.75),=
=7
CQUAD4,1,100,1,2,9,8,,-.1875
=,* (6),=,* (7),* (7),* (7),* (7),,=
=6
CQUAD4,2,100,2,3,10,9,,-.1875
=,* (6),=,* (7),* (7),* (7),* (7),,=
=6
CQUAD4,3,100,3,4,11,10,,-.1875
=,* (6),=,* (7),* (7),* (7),* (7),,=
=6
CQUAD4,4,100,4,5,12,11,,-.1875
=,* (6),=,* (7),* (7),* (7),* (7),,=
=6
CQUAD4,5,100,5,6,13,12,,-.1875
=,* (6),=,* (7),* (7),* (7),* (7),,=
=6
CQUAD4,6,100,6,7,14,13,,-.1875
=,* (6),=,* (7),* (7),* (7),* (7),,=
=6
CQUAD4,101,101,101,102,109,108,,.125
=,* (6),=,* (7),* (7),* (7),* (7),,=
=6
CQUAD4,102,101,102,103,110,109,,.125
=,* (6),=,* (7),* (7),* (7),* (7),,=
=6
CQUAD4,103,101,103,104,111,110,,.125
=,* (6),=,* (7),* (7),* (7),* (7),,=
=6
CQUAD4,104,101,104,105,112,111,,.125
=,* (6),=,* (7),* (7),* (7),* (7),,=
=6
CQUAD4,105,101,105,106,113,112,,.125
=,* (6),=,* (7),* (7),* (7),* (7),,=
=6

```

Figure B.7 MSC/NASTRAN Frequency Response Analysis
of the Simple Plate (Page Two)

```

CQUAD4,106,101,106,107,114,113,,.125
=,* (6),=,* (7),* (7),* (7),* (7),=
=6
CHEXA,201,200,1,2,9,8,101,102,+01
=,* (6),=,* (7),* (7),* (7),* (7),* (7),* (7),* (1)
=,* (6),=,* (7),* (7),* (7),* (7),* (7),* (7),* (1)
=,* (6),=,* (7),* (7),* (7),* (7),* (7),* (7),* (1)
=,* (6),=,* (7),* (7),* (7),* (7),* (7),* (7),* (1)
=,* (6),=,* (7),* (7),* (7),* (7),* (7),* (7),* (1)
=,* (6),=,* (7),* (7),* (7),* (7),* (7),* (7),* (1)
=,* (6),=,* (7),* (7),* (7),* (7),* (7),* (7),* (1)
+01,109,108
*1,*7,*7
*1,*7,*7
*1,*7,*7
*1,*7,*7
*1,*7,*7
*1,*7,*7
*1,*7,*7
*1,*7,*7
CHEXA,202,200,2,3,10,9,102,103,+09
=,* (6),=,* (7),* (7),* (7),* (7),* (7),* (7),* (1)
=,* (6),=,* (7),* (7),* (7),* (7),* (7),* (7),* (1)
=,* (6),=,* (7),* (7),* (7),* (7),* (7),* (7),* (1)
=,* (6),=,* (7),* (7),* (7),* (7),* (7),* (7),* (1)
=,* (6),=,* (7),* (7),* (7),* (7),* (7),* (7),* (1)
=,* (6),=,* (7),* (7),* (7),* (7),* (7),* (7),* (1)
=,* (6),=,* (7),* (7),* (7),* (7),* (7),* (7),* (1)
+09,110,109
*1,*7,*7
*1,*7,*7
*1,*7,*7
*1,*7,*7
*1,*7,*7
*1,*7,*7
CHEXA,203,200,3,4,11,10,103,104,+17
=,* (6),=,* (7),* (7),* (7),* (7),* (7),* (7),* (1)
=,* (6),=,* (7),* (7),* (7),* (7),* (7),* (7),* (1)
=,* (6),=,* (7),* (7),* (7),* (7),* (7),* (7),* (1)
=,* (6),=,* (7),* (7),* (7),* (7),* (7),* (7),* (1)
=,* (6),=,* (7),* (7),* (7),* (7),* (7),* (7),* (1)
=,* (6),=,* (7),* (7),* (7),* (7),* (7),* (7),* (1)
=,* (6),=,* (7),* (7),* (7),* (7),* (7),* (7),* (1)
+17,111,110
*1,*7,*7
*1,*7,*7
*1,*7,*7

```

Figure B.8 MSC/NASTRAN Frequency Response Analysis
of the Simple Plate (Page Three)

```

*1,*7,*7
*1,*7,*7
*1,*7,*7
*1,*7,*7
CHEXA,204,200,4,5,12,11,104,105,+25
=,*(6),=,*(7),*(7),*(7),*(7),*(7),*(7),*(1)
=,*(6),=,*(7),*(7),*(7),*(7),*(7),*(7),*(1)
=,*(6),=,*(7),*(7),*(7),*(7),*(7),*(7),*(1)
=,*(6),=,*(7),*(7),*(7),*(7),*(7),*(7),*(1)
=,*(6),=,*(7),*(7),*(7),*(7),*(7),*(7),*(1)
=,*(6),=,*(7),*(7),*(7),*(7),*(7),*(7),*(1)
=,*(6),=,*(7),*(7),*(7),*(7),*(7),*(7),*(1)
+25,112,111
*1,*7,*7
*1,*7,*7
*1,*7,*7
*1,*7,*7
*1,*7,*7
*1,*7,*7
*1,*7,*7
CHEXA,205,200,5,6,13,12,105,106,+33
=,*(6),=,*(7),*(7),*(7),*(7),*(7),*(7),*(1)
=,*(6),=,*(7),*(7),*(7),*(7),*(7),*(7),*(1)
=,*(6),=,*(7),*(7),*(7),*(7),*(7),*(7),*(1)
=,*(6),=,*(7),*(7),*(7),*(7),*(7),*(7),*(1)
=,*(6),=,*(7),*(7),*(7),*(7),*(7),*(7),*(1)
=,*(6),=,*(7),*(7),*(7),*(7),*(7),*(7),*(1)
=,*(6),=,*(7),*(7),*(7),*(7),*(7),*(7),*(1)
+33,113,112
*1,*7,*7
*1,*7,*7
*1,*7,*7
*1,*7,*7
*1,*7,*7
*1,*7,*7
CHEXA,206,200,6,7,14,13,106,107,+41
=,*(6),=,*(7),*(7),*(7),*(7),*(7),*(7),*(1)
=,*(6),=,*(7),*(7),*(7),*(7),*(7),*(7),*(1)
=,*(6),=,*(7),*(7),*(7),*(7),*(7),*(7),*(1)
=,*(6),=,*(7),*(7),*(7),*(7),*(7),*(7),*(1)
=,*(6),=,*(7),*(7),*(7),*(7),*(7),*(7),*(1)
=,*(6),=,*(7),*(7),*(7),*(7),*(7),*(7),*(1)
=,*(6),=,*(7),*(7),*(7),*(7),*(7),*(7),*(1)

```

Figure B.9 MSC/NASTRAN Frequency Response Analysis
of the Simple Plate (Page Four)

```

+41,114,113
*1,*7,*7
*1,*7,*7
*1,*7,*7
*1,*7,*7
*1,*7,*7
*1,*7,*7
*1,*7,*7
DLOAD,2000,1.0,1.0,2001
RLOAD1,2001,2002,,,2003
DAREA,2002,40,3,1.
TABLED1,2003,,,,,,,,+TA
+TA,0.,1.,5000.,1.0,ENDT
FREQ1,2100,450.,5.,20
PSHELL,100,100,.375,100
PSHELL,101,100,.25,100
PSOLID,200,200,0
MAT1,100,1.+7,.,33,.0955
MAT1,200,.,2354.02,.49,.035,,,1.089
PARAM,ASING,1
PARAM,AUTOSPC,YES
SPC1,10,6,101,THRU,163
SPC1,10,6,1,THRU,63
SUPT,32,12345
EIGR,1,MGIV,1.,1500.,,20,,,+ZZ
+ZZ,MASS
PARAM,WTMASS,.00259
ENDDATA

```

Figure B.10 MSC/NASTRAN Frequency Response Analysis
of the Simple Plate (Page Five)

LIST OF REFERENCES

1. Meirovitch, L., Elements of Vibration Analysis, McGraw-Hill Book Company, 1986.
2. Gockel, M.A. (Ed.), MSC/NASTRAN Handbook for Dynamic Analysis, McNeal-Schwendler Corp., Los Angeles, California, June 1983.
3. Buhasiwalu, K.J. and Hansen, J.S., "Dynamics of Viscoelastic Structure Structures," Damping 1986 Proceedings, Flight Dynamics Laboratory, Air Force Wright Aeronautical Laboratories, Air Force System Command, Wright-Patterson Air Force Base, Ohio.
4. Frater, N.K., "Implementation of Modal Strain Energy Method Using MSC/NASTRAN and Postprocessing Utility Programs," Damping 1986 Proceedings, Flight Dynamics Laboratory, Air Force Wright Aeronautical Laboratories, Air Force System Command, Wright-Patterson Air Force Base, Ohio.
5. Nashif, Jones, and Henderson, Vibration Damping, Wiley-Interscience Publications, John Wiley and Sons, 1985.
6. University of Dayton Research Institute, "Selected UDRI Evaluated Material Properties," Vibration Damping Short Course Notes, University of Dayton, Ohio.
7. Johnson, C.D. and Kienholz, D.A., "Finite Element Damping in Structures with Constrained Viscoelastic Layers," Report No. 82.053, May 1982.
8. Drake, M.L., "Design Techniques Fourth Order Beam Theory," Vibration Damping Short Course Notes, University of Dayton, Ohio.
9. Ross, D., Ungar, E.E., and Kerwin, E.M., "Damping of Plate Flexured Vibrations by Means of Viscoelastic Laminar," Damping 1986 Proceedings, Flight Dynamics Laboratory, Air Force Wright Aeronautical Laboratories, Air Force System Command, Wright-Patterson Air Force Base, Ohio.
10. Course notes from Vibration Short Course given by the University of Dayton Research Institute, Dayton, Ohio, June 1987, M.L. Drake, Course Director.

11. Reinhall, P.G., Miles, R.N., "Effects of Bond Imperfections on the Dynamic Response of Laminated Beams," Damping 1986 Proceedings, Flight Dynamics Laboratory, Air Force Wright Aeronautical Laboratories, Air Force System Command, Wright-Patterson Air Force Base, Ohio.
12. David, I.G., Jones and Henderson, J.P., "Fundamentals of Damping Materials," Vibration Damping Short Course Notes, University of Dayton, Ohio.
13. Joseph, J.A. (Ed.), MSC/NASTRAN Application Manual, Vol. 1, McNeal-Schwendler Corp., Los Angeles, California, March 1977.
14. Killian, J.W., Lu, Y.P., "A Finite Element Modeling Approximation for Damping Material Used in Constrained Damped Structures," Journal of Sound Vibration (1984) 97(2).

INITIAL DISTRIBUTION LIST

	No. Copies
1. Defense Technical Information Center Cameron Station Alexandria, Virginia 22304-6145	2
2. Library, Code 0142 Naval Postgraduate School Monterey, California 93943-5002	2
3. Dean of Science and Engineering, Code 06 Naval Postgraduate School Monterey, California 93943-5004	2
4. Research Administrations Office, Code 012 Naval Postgraduate School Monterey, California 93943-5004	1
5. Department Chairman, Code 69 Department of Mechanical Engineering Naval Postgraduate School Monterey, California 93943-5004	1
6. Professor Y.S. Shin, Code 69Sg Department of Mechanical Engineering Naval Postgraduate School Monterey, California 93943-5004	3
7. Dr. K.S. Kim, Code 69Ki Department of Mechanical Engineering Naval Postgraduate School Monterey, California 93943-5004	1
8. Dr. Arthur Kilcullen, Code 1962 David W. Taylor Naval Ship R&D Center Bethesda, Maryland 20084	5
9. Mrs. Kathy Wong, Code 2812 David W. Taylor Naval Ship R&D Center Annapolis, Maryland 21402	1
10. Mr. Robert Hardy, Code 2803 David W. Taylor Naval Ship R&D Center Annapolis, Maryland 21402	1

- | | |
|--|---|
| 11. Dr. D.J. Vendittis, Code 196
David W. Taylor Naval Ship R&D Center
Ship Acoustics Department (196)
Bethesda, Maryland 20084 | 1 |
| 12. Mr. V.J. Castelli, Code 2844
David W. Taylor Naval Ship R&D Center
Annapolis, Maryland 21402 | 1 |
| 13. Professor J. Perkins, Code 69Ps
Department of Mechanical Engineering
Naval Postgraduate School
Monterey, California 93943-5004 | 1 |
| 14. Dr. B. Whang, Code 1750.2
David W. Taylor Naval Ship R&D Center
Hull Group Head, Submarine Protection Div.
Bethesda, Maryland 20084 | 1 |
| 15. Dr. N.T. Tsai
Defense Nuclear Agency
SPSS
Washington, D.C. 20305-1000 | 1 |
| 16. Dr. P. Mahmoodi
3M-3M Center
Corporate Research Laboratories/3M
Bldg. 201-BS-08
St. Paul, Minnesota 55144-1000 | 1 |
| 17. Mr. Gerald Maurer
22221 County Road 43
Big Lake, Minnesota 55309 | 3 |

END

DATE

FILMED

6-1988

DTIC